CDF/ANAL/EXOTIC/GROUP/8316
Draft 0.1
August 17, 2006

Anomalous Production of Z-Bosons with High Transverse Momentum in 0.94 fb^{-1} at the Tevatron

Alexander Paramonov[1] and Henry Frisch[2]

Enrico Fermi Institute, University of Chicago

Abstract

We update our previous note, CDF8033, to have the full 0.94 fb^{-1} of data. We have also looked in additional signatures associated with the production of Z-bosons. As before, we consider Z-bosons with high transverse momenta ($P_T(Z)$) as the signal region. The new signatures considered are Z + X + anything and Z + X + Y + anything, where X and Y can be leptons, photons, missing energy, or large total transverse energy (H_T). For every given signature we compare the observed $P_T(Z)$ spectra and other distributions with Standard Model expectations. Alas, we do not see anything striking.

[1]paramon@hep.uchicago.edu
[2]frisch@hep.uchicago.edu

Contents

1 Introduction

This paper is an update for CDF Note 8033, which should be read first.

The Standard Model (SM) is the most successful theory describing the interactions of elementary particles. However, even this theory has some unsolved problems such as a large number of constants, the existence of the Higgs particle, Grand Unification, Super-symmetry, and flavor and CP violations. Many Standard Model extensions face solving these difficulties. Most of these SM extensions introduce new heavy particles coupled to the electroweak sector. These particles decay producing gauge bosons (W's and Z's) with large transverse momenta (P_T). This paper presents a signature-based method [1, 2] for searching for new heavy particles based on their weak decays. In the analysis presented here the observed P_T spectra of inclusive Z's are compared to SM-predicted backgrounds.

The CDF II Detector at the Fermilab Tevatron is an azimuthally and forward-backward symmetric spectrometer designed to study $p\overline{p}$ collisions at $\sqrt{s} = 1.96$ TeV. This is a general purpose solenoidal detector which combines precision charged particle tracking with fast projective calorimetry and fine-grained muon chambers. Tracking systems are enclosed in a superconducting solenoid which generates a 1.4 T magnetic field parallel to the beam axis. Calorimeters and muon systems are outside the solenoid. The present study employs leptonic decays of W's and Z's using data collected at CDF Run II at the Tevatron from 2001 to February of 2006. Technical details of the detector are described elsewhere [3].

The collisions of protons and anti-protons occur every 396 ns with $\sqrt{s} = 1.96$ TeV. To select collisions of interest (events) from this enormous flow a sophisticated triggering and data acquisition system is used. In this analysis we observe events triggered with high-P_T leptons (electrons and muons).

Monte Carlo (MC) samples of SM processes are used to predict the observed P_T spectra. We use MC samples of Z + jets, $t\bar{t}$, diboson (WW, WZ, ZZ, and Zγ), and $Z^0 \to \tau^+\tau^-$ in the analysis. Contributions from 'fake' electrons and muons are estimated with data.

2 Search Strategy

We present a broad signature-based search for inclusive high-P_T Z's coming from decays of new heavy particles such as Z', Q_R, etc. The Z bosons are reconstructed in $Z \to ee$ and $Z \to \mu\mu$ decay modes.

The search strategy includes three stages:

- In the first stage we consider inclusive Z-production.

- In the second stage we select events where the Z is produced in association with X: Z+X+anything. The symbol X stands for any reconstructed object such as a lepton (e or μ), a photon, high transverse momenta, or the signature of missing transverse energy.

- In the third stage we study Z+X+Y+anything. In this case X and Y can be any of the above (nonidentical) reconstructed objects (multiple identical objects will show up in the plots in the Z+X search).

In the first stage, inclusive Z production, the observed events are split into three control samples to compare the underlying event structure at different $P_T(Z)$ scales:

- Inclusive Z's,
- Z's with $P_T(Z) > 60$ GeV,
- Z's with $P_T(Z) > 120$ GeV.

The observed distributions in a number of variables are then compared with Standard Model predictions calculated using a tuned CDF version of the PYTHIA Monte-Carlo generator [4]. We also set a limit on the anomalous production of inclusive Z's at 95% CL, assuming the new physics has the same acceptance as Standard Model Z-bosons production. Also we combine the limits into one.

The missing energy signature ($\not\!\!E_{\mathrm{T}}$-signature) is a combination of cuts:

$$\not\!\!E_{\mathrm{T}} > 25 \text{ GeV and } (H_T < 150 \text{ GeV or } \not\!\!E_{\mathrm{T}}\text{-significance} > 3).$$

Definitions of the $\not\!\!E_{\mathrm{T}}$ and the H_T can be found in the next section. We use the following equations to calculate $\not\!\!E_{\mathrm{T}}$-significance:

$$\not\!\!E_{\mathrm{T}} - significance = \frac{\not\!\!E_{\mathrm{T}}}{\sigma(\not\!\!E_{\mathrm{T}})} \tag{1}$$

$$\sigma^2(\not\!\!E_{\mathrm{T}}) = \Sigma\sigma^2_{jet} + \Sigma\sigma^2_{e/\gamma} + \Sigma\sigma^2_{\mu} \tag{2}$$

The sums are calculated for all the reconstructed objects in event.
Jets:

$$\frac{\sigma_{jet}}{E_T(jet)} = \frac{80\%}{\sqrt{E_T(jet)}} \oplus 4\% \tag{3}$$

CEM electrons and photons:

$$\frac{\sigma_{e/\gamma}}{E_T} = \frac{13.5\%}{\sqrt{E_T}} \oplus 2\% \tag{4}$$

PEM electrons and photons:

$$\frac{\sigma_{e/\gamma}}{E_T} = \frac{14.4\%}{\sqrt{E_T}} \oplus 0.7\% \tag{5}$$

Muons:

$$\frac{\sigma_\mu}{P_T(\mu)} = 0.091\% * P_T(\mu) \tag{6}$$

Please note that this definition of $\not\!\!E_{\mathrm{T}}$-significance does not use total energy deposited in the calorimeter and so it is not affected by min-bias events. Some fraction of this total energy is unclustered and partially comes from min-bias (underlying) events. (The Monte Carlo samples we use do not include the min-bias events and this is the reason why we apply the $H_T > 150$GeV cut in the $\not\!\!E_{\mathrm{T}}$-signature.) Distributions of the $\not\!\!E_{\mathrm{T}}$-significance are in the Fig. 1 and Fig. 2.

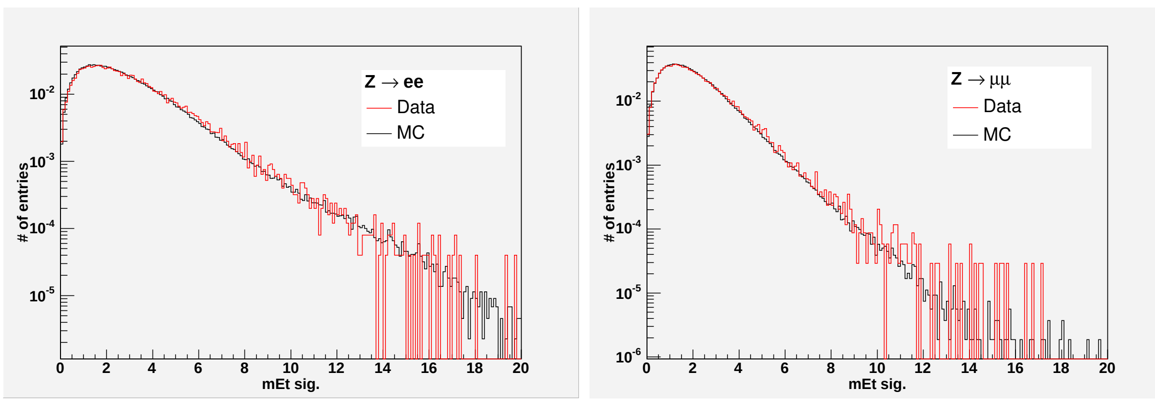

Figure 1: $\not\!\!E_{\mathrm{T}}$-significance comparison between Data and MC for $Z \to \mu\mu$ events (right) and $Z \to ee$ events (left).

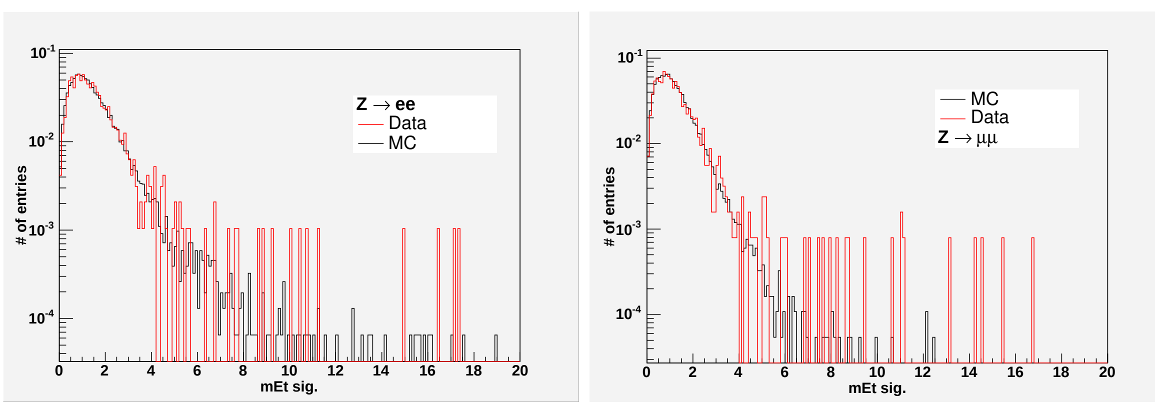

Figure 2: $\not\!\!E_{\mathrm{T}}$-significance comparison between Data and MC for $Z \to \mu\mu$ (right) and $Z \to ee$ (left) in events with $H_T > 150$ GeV.

3 Data Selection

We follow the same data selection procedure as in CDF Note 8033.

Events with inclusive Z-bosons (Z+ anything) are selected using high-P_T electrons and muons in the leptonic decay channels $Z \rightarrow ee$ and $Z \rightarrow \mu\mu$. The reconstructed invariant mass of a leptonic pair is required to be in the mass window from 66 GeV to 116 GeV.

In order to check that the SM modeling represents the data in the broad range of $P_T(z)$ below the very high-P_T region of interest, events with Z's are split into 3 categories:

- Inclusive Z's
- Events with $P_T(Z) > 60$ GeV.
- Events with $P_T(Z) > 120$ GeV.

The numbers of the observed $Z \rightarrow ee$ and $Z \rightarrow \mu\mu$ decays in each category are presented in Table 1.

The observed events are triggered on high-P_T electrons and muons selected by the ELECTRON_CENTRAL_18, MUON_CMUP_18, and MUON_CMX_18 triggers, respectively. We require the SVX detector to be functional by taking events from the silicon Good Run list, V13, defined by the DQM group (the bits are (1,1,1,1)). The electron datasets (bhel0d, bhel0h, and bhel0i) contain 33,706,930 events and correspond to an integrated luminosity of 0.94 fb^{-1} . The muon datasets (bhmu0d, bhmu0h, and bhmu0i) have 15,829,290 events and correspond to a luminosity of 0.94 fb^{-1} .

The data were kindly accumulated by the CDF II collaboration at the Tevatron.

Details of the reconstruction of W and Z bosons are described below:

- $Z \rightarrow ee$ events are reconstructed using a tight CEM electron (see Table 3) and a loose CEM electron (see Table 3). A tight CEM electron passes all the loose cuts. A histogram of the $Z \rightarrow ee$ invariant mass is shown in Figure 3.
- The $Z \rightarrow \mu\mu$ event selection requires a tight and a loose muon (see Table 2). The observed invariant mass histogram is shown in Figure 11.

The kinematic structure of the events is studied from the distributions in the following variables:

- H_T (Scalar sum of E_T of all reconstructed objects (electrons, muons, jets, and missing transverse energy)),
- Missing transverse energy ($\not\!\!E_{\mathrm{T}}$) (Negative vector sum of $\vec{E}_T$ of all reconstructed objects (electrons, muons, photons, and jets)),
- Number of jets. Jets are reconstructed with Level 5 corrections and required to satisfy $E_T > 15$ GeV and $|\eta| < 2.4$,
- Number of photons (Photon ID cuts are described in Table 5.),

- Number of extra leptons (tight electrons and muons which are not used in reconstruction of Z-boson).

Electrons in the end-plug regions (Plug electrons) are used only in the calculations of $\mathrm{H_T}$ and $\not{E}_\mathrm{T}$. The selection cuts for the Plug electrons are listed in Table 4.

Decay mode of the Z-boson	Inclusive	$P_T(Z) > 60$ GeV	$P_T(Z) > 120$ GeV
$Z \to ee$	25079	587	70
$Z \to \mu\mu$	34222	721	74

Table 1: Number of the inclusive Z's observed in $Z \to ee$ and $Z \to \mu\mu$ decay modes.

Variable	Tight	Loose
P_T, GeV	> 20	> 12
E_{EM}, GeV	$<$ 2+max(0,p-100)$*$0.0115	$<$ 2+max(0,p-100)$*$0.0115
E_{HAD}, GeV	$<$ 6+max(0,p-100)$*$0.028	$<$ 6+max(0,p-100)$*$0.028
$isolation/P_T$	< 0.1	< 0.1
#SL with ≥ 5 hits	≥ 3 stereo and axial	≥ 3 axial and ≥ 2 stereo
χ^2_{COT}/DOF	< 3	< 4
$\|Z0\|$, cm	< 60	< 60
ΔX_{CMU}, cm	< 3	
ΔX_{CMP}, cm	< 7 (MC should be fixed!)	
ΔX_{CMX}, cm	< 6 for run > 150144	
COT exit radius	> 140 cm	
Muon Detector	CMUP or CMX	
Cosmic	No	No

Table 2: Summary of the muon cuts. See [5]. "DOF" stands for degrees of freedom (i.e. number of COT hits - 5). Fiducial cuts are not applied.

We apply Larry's corrections [6] to all tracks in data.

Variable	Tight	Loose
E_T, GeV	> 20	> 12
X_{CES}, cm		< 21
Z_{CES}, cm		< 230 and > 9
Track P_T, GeV	> 10	> 10
Track $Z0$, cm	< 60	< 60
E/P	< 2 or $P_T > 50$ GeV	
charge signed ΔX, cm	< 1.5 and $>$ -3.0	
# of Sl with ≥ 5 hits	≥ 3 axial and stereo	≥ 3 axial and stereo
Conversion	No	No
Had/EM	$< 0.055 + 0.00045{*}$E	$< 0.055 + 0.00045{*}$E
Lshr	$< .2$	
χ^2_{strip}	< 10	
Calorimeter Iso./E_T	$< .1$	$< .1$

Table 3: Summary of central (CEM) electron cuts. See [7] and [8].

Variable	Cut
E_T, GeV	> 12
$\lvert\eta_{det}\rvert$	$1.2 < \lvert\eta_{det}\rvert < 2.5$
Track type	phoenix
Track $Z0$, cm	< 60
SVX Hits	> 2
Had/EM	< 0.05
χ^2_{tree}	< 10
Frac. Cal. Iso.	$< .1$
PES 5X9 U	> 0.65
PES 5X9 V	> 0.65
PEM fit towers	$\neq 0$

Table 4: Summary of plug (PEM) electron cuts. See [9].

Variable	Cut
Corrected Et, GeV	> 25
CES X and Z Fiducial	Ces $\|X\| < 21$ cm, $9 <$ Ces $\|Z\| < 230$ cm
Had/Em	$< 0.125 \|\| < 0.055 + 0.00045$ * ECorr
Cone 0.4 IsoEtCorr (new correction- see notes)	EtCorr<20: < 0.1*EtCorr EtCorr>20: < 2.0+0.02*(EtCorr-20.0)
Chi2 (Strips+Wires)/2.0	< 20
N track (N3D)	≥ 1
Track Pt	< 1+0.005*EtCorr GeV
Cone 0.4 Track Iso	< 2.0+0.005*EtCorr
2nd CES cluster E*sin(theta) (both strip and wire E individually)	EtCorr<18: < 0.14*EtCorr EtCorr>18: < 2.4+0.01*EtCorr

Table 5: Summary of cuts for Central Photons. See [10].

4 Monte Carlo Predictions: Standard Model

The Standard Model production of inclusive Z's is modeled by means of the leading order (LO) Pythia Monte-Carlo (MC) generator [11]. The following Gen5 MC samples are used in the analysis:

- Z + jets (Drell-Yan process), where the Z decays to e^+e^-, $\mu^+\mu^-$, or $\tau^+\tau^-$
- Diboson: WW, WZ, ZZ, and Zγ (The Zγ process is included in the regular "Z + jets" sample by PYTHIA)
- $t\bar{t}$

The Z + jets datasets are produced using Pythia V6.2 [11] with the requirement that $M(\gamma^*/Z) > 30$ GeV. Tune A and the 'Willis Sakumoto' corrections have been applied.

The MC contributions from the various SM processes are combined into inclusive samples using weights proportional to the NLO cross-sections of each contribution. These summed MC-samples are then scaled to the corresponding numbers of the observed events in the $Z \to ee$ and $Z \to \mu\mu$ decay modes separately.

The MC samples were processed with the CDF "realistic" simulation (i.e. generated events were assigned real run numbers proportionally to the luminosities of the runs. This is intended to help model the operation of the SVX detector more precisely.). More detailed information regarding the MC samples is presented in Table 6.

The MC samples are studied with the same analysis routines as are the data and the same selection cuts are applied. The distributions in the dilepton invariant mass, $M_{inv}(\gamma^*/Z)$, predicted with the MC datasets are shown in the Figures 3 and 11 for the $Z \to ee$ and $Z \to \mu\mu$ decay modes, respectively. The numbers of events expected in each $P_T(Z)$-category are listed in Table 7.

SM Process	# of events	Cross Section, pb (NLO)	Comments (ID)
Z + jets, $Z \to \mu\mu$	4605792	327.8	ztop8i + ztopci
Z + jets, $Z \to ee$	5272363	327.8	ztop7i + ztopbi
Z + jets, $Z \to \tau\tau$	1222320	327.8	ztop4i
ZZ	412866	1.55 $\pm$ 0.002	ztopcz
WZ	412866	3.96 $\pm$ 0.006	wtop1z
WW	412866	13.25 $\pm$ 0.025	wtop1w
$t\bar{t}$	1146088	6.7 $\pm$ 0.07	ttopel

Table 6: Summary of the Pythia MC datasets used in the analysis. The corresponding total luminosities of the $Z \to ee$ and $Z \to \mu\mu$ MC-datasets are about 15 fb^{-1} each.

In addition to the described MC samples we have samples of inclusive $Z \to ee$ and $Z \to \mu\mu$ events in which the Z-bosons are produced with $P_T(Z) > 100$ GeV. These high-P_T samples are used to calculate P_T-dependent distribution of acceptance*efficiency of the Z-bosons.

Decay mode of the Z-boson	Inclusive	$P_T(Z) > 60$ GeV	$P_T(Z) > 120$ GeV
$Z \to ee$	25079	500	53.7
$Z \to \mu\mu$	34222	650	61.8

Table 7: Number of the inclusive Z's expected in $Z \to ee$ and $Z \to \mu\mu$ decay modes.

4.1 Energy resolution and Scale factors for MC events

The used MC's have too optimistic predictions of energy and momentum resolution of tracks and CEM clusters. The procedure of obtaining a better agreement is following:

- We smear track momentum: $1/P_T \to 1/P_T$ + Gauss(0, 0.000475)[3]. (See Daniel's CDF Note for more details).
- Energy of the electrons is corrected also: $E_T \to 0.996{*}E_T$ + Gauss(0, 0.002).

We do not apply any scale factors to the generated$Z \to ee$ events. However, we do weight generated CMUP muons by 0.923 to calculate acceptance*efficiency of reconstruction of the Z^0-bosons.

5 Backgrounds from fake Z-bosons

5.1 Hadron Jet Backgrounds

This background consists of events in which one or more leptons are "fake", i.e. jets misidentified as leptons. We expect that in our samples the two fake leptons, or, less often, one real lepton and one fake lepton, making up the Z in the background events have no charge correlation [4]. This assumption means that the number of same-sign and opposite-sign pairs are about equal. Therefore, we use the number of the same sign lepton pairs to estimate the hadron jet background in the $\gamma^*/Z^0 \to l^+l^-$ sample.

The $Z \to \mu\mu$ sample (66 GeV $< M_{inv}(ll) <$ 116 GeV) contains only 2 events with muons of the same sign.

The number of same-sign electron pairs in the $Z \to ee$ sample is corrected for the number of real e^+e^- pairs mis-reconstructed as e^+e^+ or e^-e^- using the MC predictions for $Z \to ee$ production.

We observe 272 same-sign electron pairs corresponding to 25079 e^+e^- pairs. We remove the contribution of real $\gamma^*/Z^0 \to e^+e^-$ events from the number of observed events by subtracting the number of observed e^+e^- events scaled by fraction of same-sign to opposite-sign events in the Monte-Carlo samples for $Z \to ee$. The remaining number of the same-sign electron pairs is used to estimate the hadron jet background in the $Z \to ee$ sample (see Fig. 3).

[3]By Gauss(x, y) we imply a random number which is distributed normally with average of x and dispersion of y

[4]There is a charge correlation in W+1jet with the jet faking a lepton- this background is small here.

5.2 Electroweak Backgrounds

Several electroweak processes mimic $\gamma^*/Z^0 \rightarrow l^+l^-$ production. The processes are $Z^0 \rightarrow \tau^+\tau^-$, W^+W^-, and $t\bar{t}$ production. Their contributions to γ^*/Z^0 production are estimated from the corresponding MC-simulated samples. The MC simulations are based on the Standard Model predictions.

5.3 Cosmic Ray Backgrounds

High-energetic cosmic muons traverse the CDF detector at some significant rate and reconstructed as $\mu^+\mu^-$ pairs. We remove the cosmic muons with the cosmic ray tagging algorithm (See [12]) which basically fits the two tracks of the $\mu^+\mu^-$ pair with a single arc. If the fit is successful, the muon pair is tagged as cosmic muons and removed from the $Z \rightarrow \mu\mu$ sample [12]. The algorithm is $99.75 \pm 0.05\%$ efficient and the mistag rate is $0.03 \pm 0.02\%$. The number of cosmic muons estimated from the distribution of $|\vec{P}(Z)|$ is 0 (Cosmic $\mu^+\mu^-$ pairs have a peak at 0 GeV and real $Z \rightarrow \mu\mu$ decays have negligibly small phase space at low $|\vec{P}(Z)|$).

6 Control Samples: Z Production; MC and Data

The distributions for the variables characterizing the underlying event structure are shown below. The figures contain three histograms for the samples with different cuts on the transverse momentum of the Z boson. Good agreement of data and SM predictions is observed at different $P_T(Z)$ scales. We expect that the MC predictions of the $P_T(Z)$ distribution to be modeled correctly for the whole P_T range.

6.1 $Z \to ee$ sample.

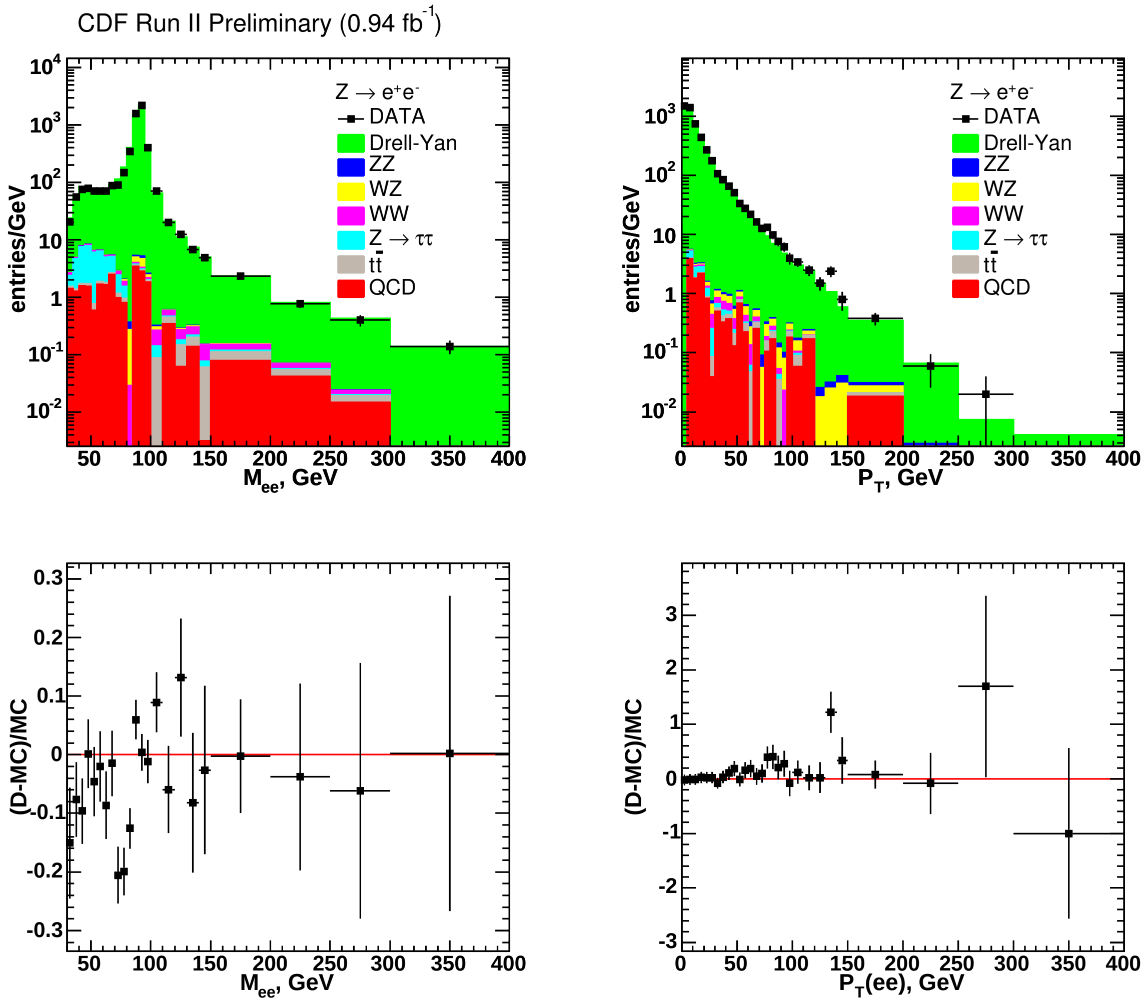

Figure 3: Invariant mass (left) and transverse momentum (right) for $Z \to ee$. The two lower plots show the difference between the numbers of expected and observed events divided by the number expected. A mass cut of 66 < M(ee) < 116 GeV has been applied to the right-hand plot.

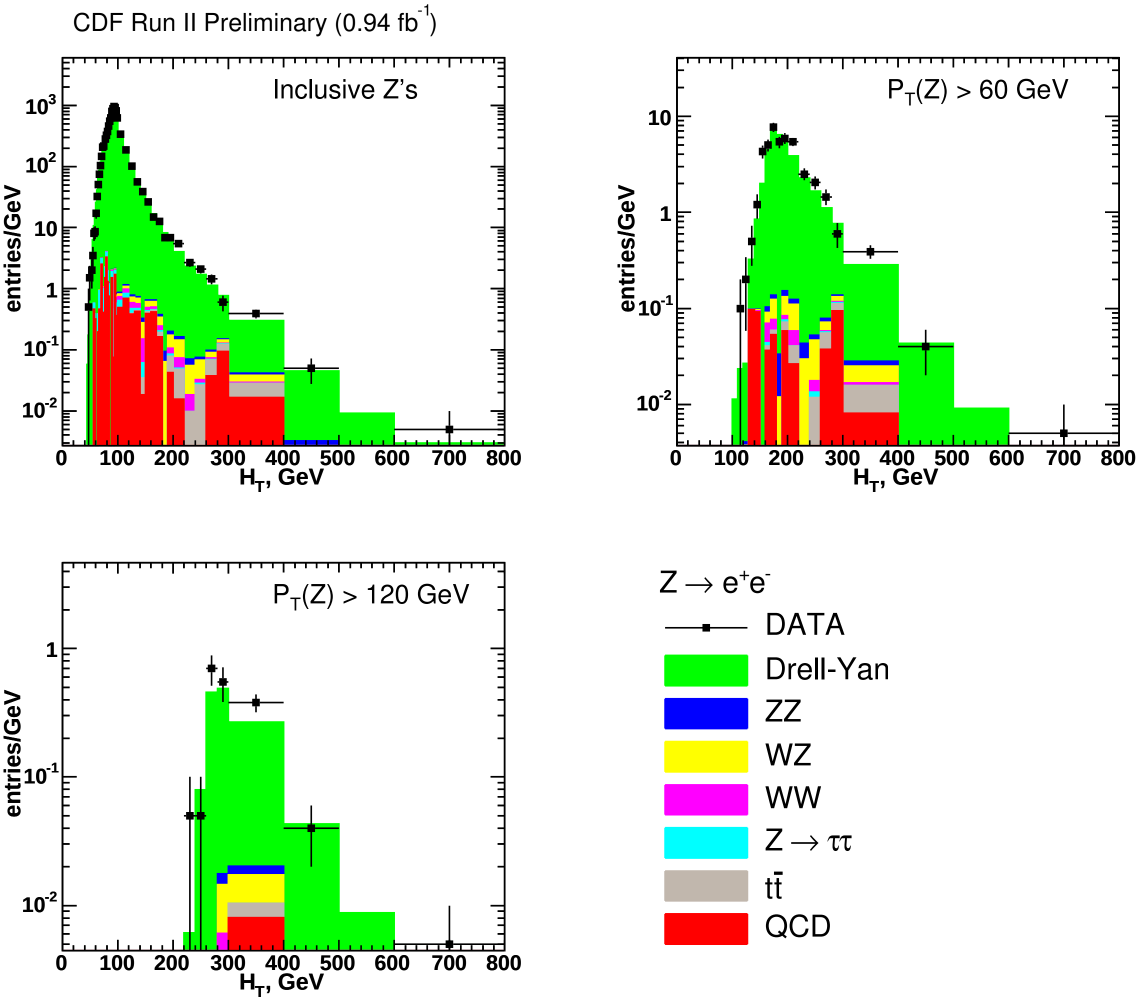

Figure 4: A comparison of H_T (scalar sum of E_T over all objects in an event)for the $Z \to ee$ data and SM MC. The distributions are calculated for three subsamples of $Z \to ee$ with different cuts on $P_T(Z) >$: 0 GeV, 60 GeV, and 120 GeV. The mass cut of 66 < M(ee) < 116 GeV has been applied.

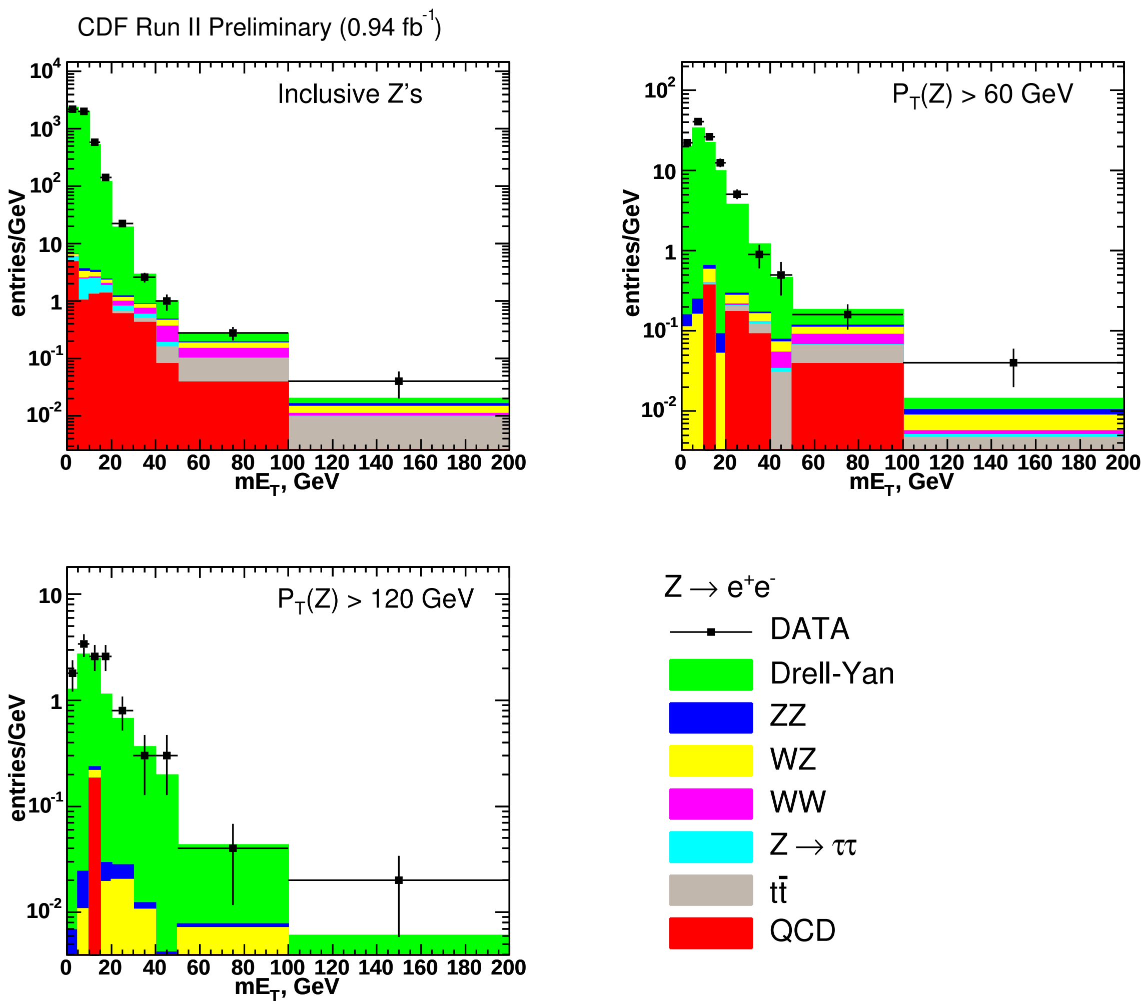

Figure 5: The measured distributions for $\not{E}_{\mathrm{T}}$ are compared to SM expectations for three subsamples of $Z \to ee$ with different cuts on $P_T(Z) >$: 0 GeV, 60 GeV, and 120 GeV. The mass cut of 66 < M(ee) < 116 GeV has been applied.

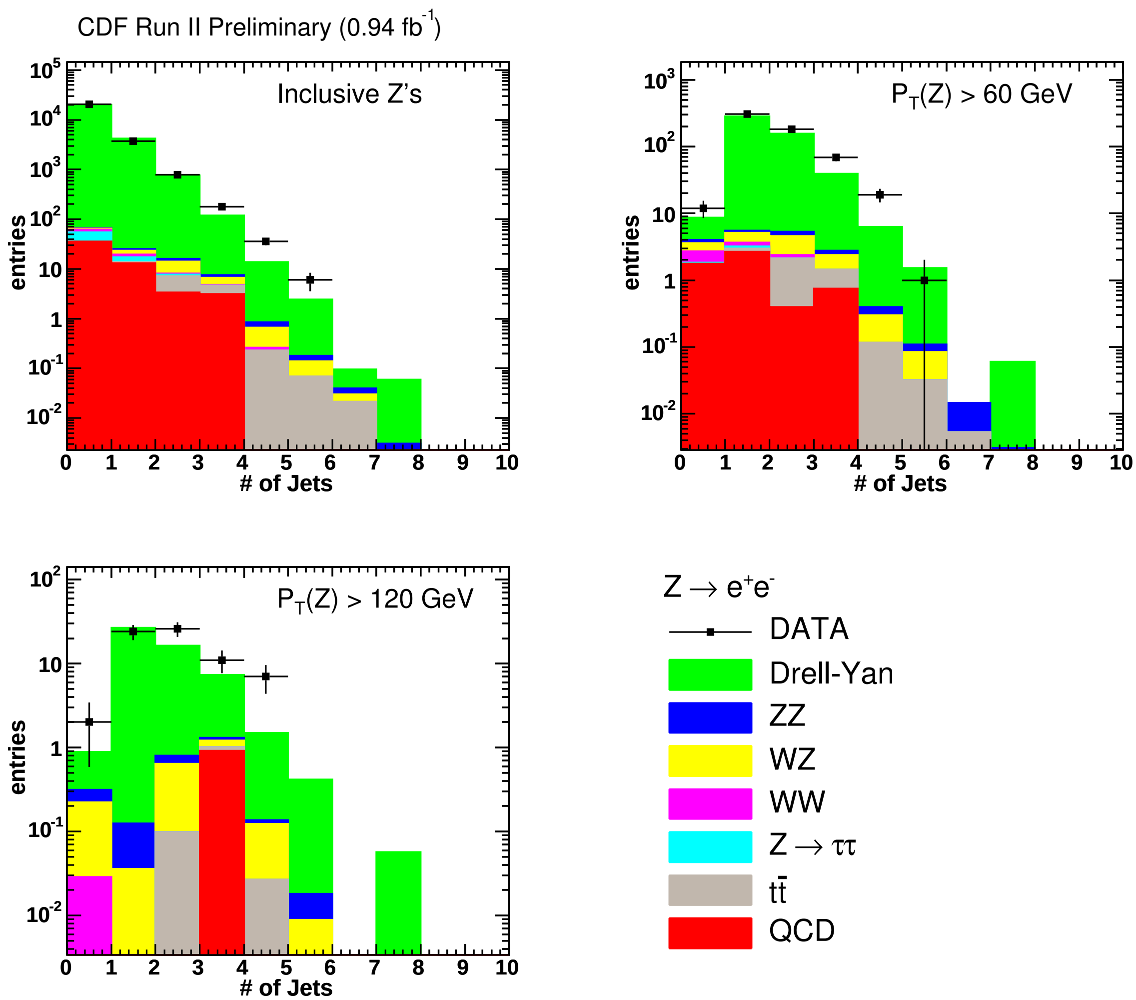

Figure 6: The measured distributions for the number of jets in data compared to SM expectation for the subsamples of $Z \to ee$ with $P_T(Z)$ cuts ($>$ 0 GeV, $>$ 60 GeV, and $>$ 120 GeV). The mass cut of 66 $<$ M(ee) $<$ 116 GeV has been applied.

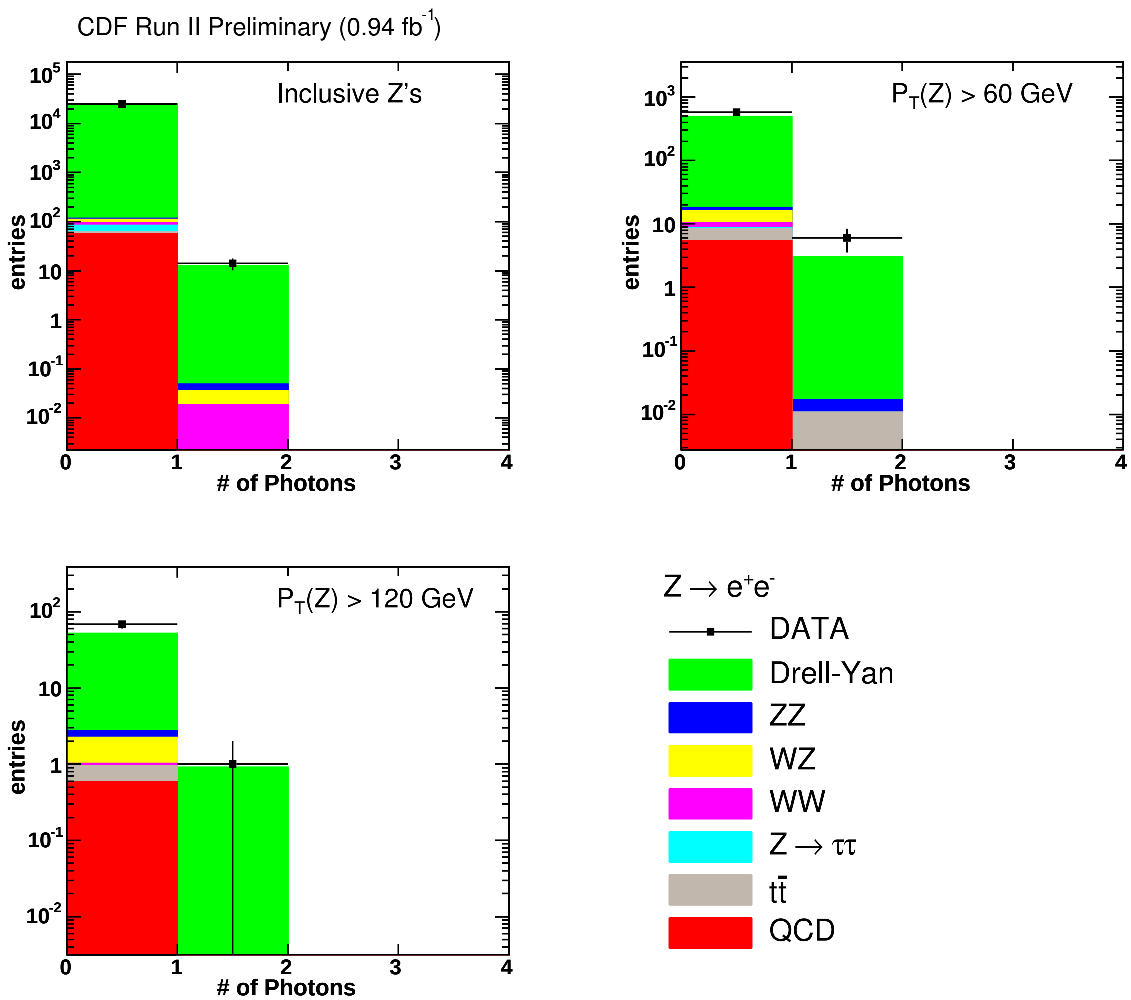

Figure 7: The measured distributions for the numbers of photons in data compared to SM expectations for $Z \rightarrow ee$ subsamples $P_T(Z)$ cuts ($>$ 0 GeV, $>$ 60 GeV, and $>$ 120 GeV). The mass cut of 66 $<$ M(ee) $<$ 116 GeV has been applied.

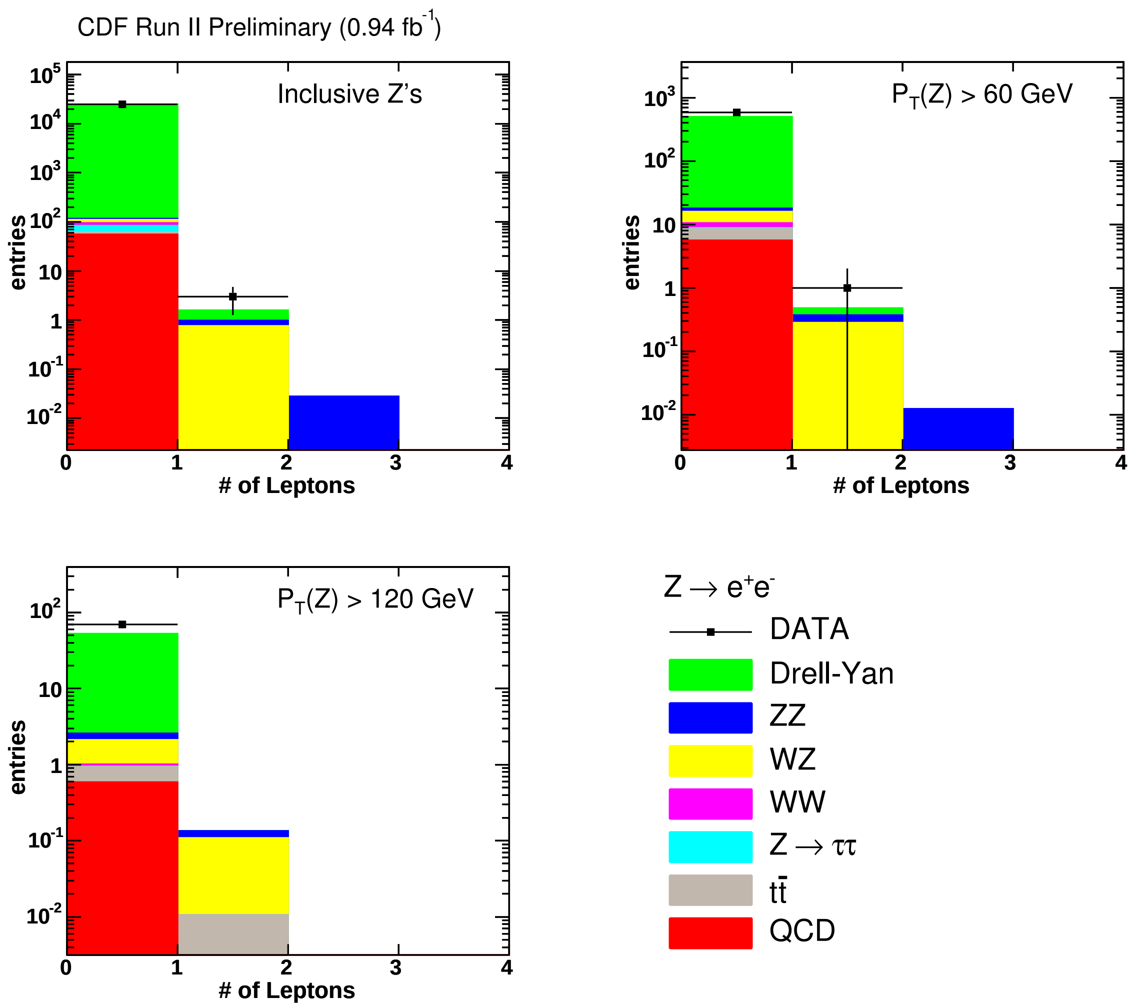

Figure 8: The measured distributions for the number of leptons in data compared to the SM expectations for the $Z \to ee$ samples with different $P_T(Z)$ cuts. The mass cut of $66 < \mathrm{M(ee)} < 116$ GeV has been applied.

$cos(\alpha)$ represent cos of the angle between positively charged lepton and the direction of $\vec{P}(Z)$ in the rest frame of the Z-boson. The $\vec{P}(Z)$ is calculated in the rest frame of CDF. We used the following formula to calculate $cos(\alpha)$:

$$cos(\alpha) = \frac{E_1 - E_2}{P(Z)} * q_1. \tag{7}$$

The E_i are the energies of the leptons in the rest frame of CDF (i = 1,2) and q_1 is the charge of the 1st lepton in units of the electron charge (i.e. $q_1^2 = 1$). Please call me[5] if you find that the formula is wrong.

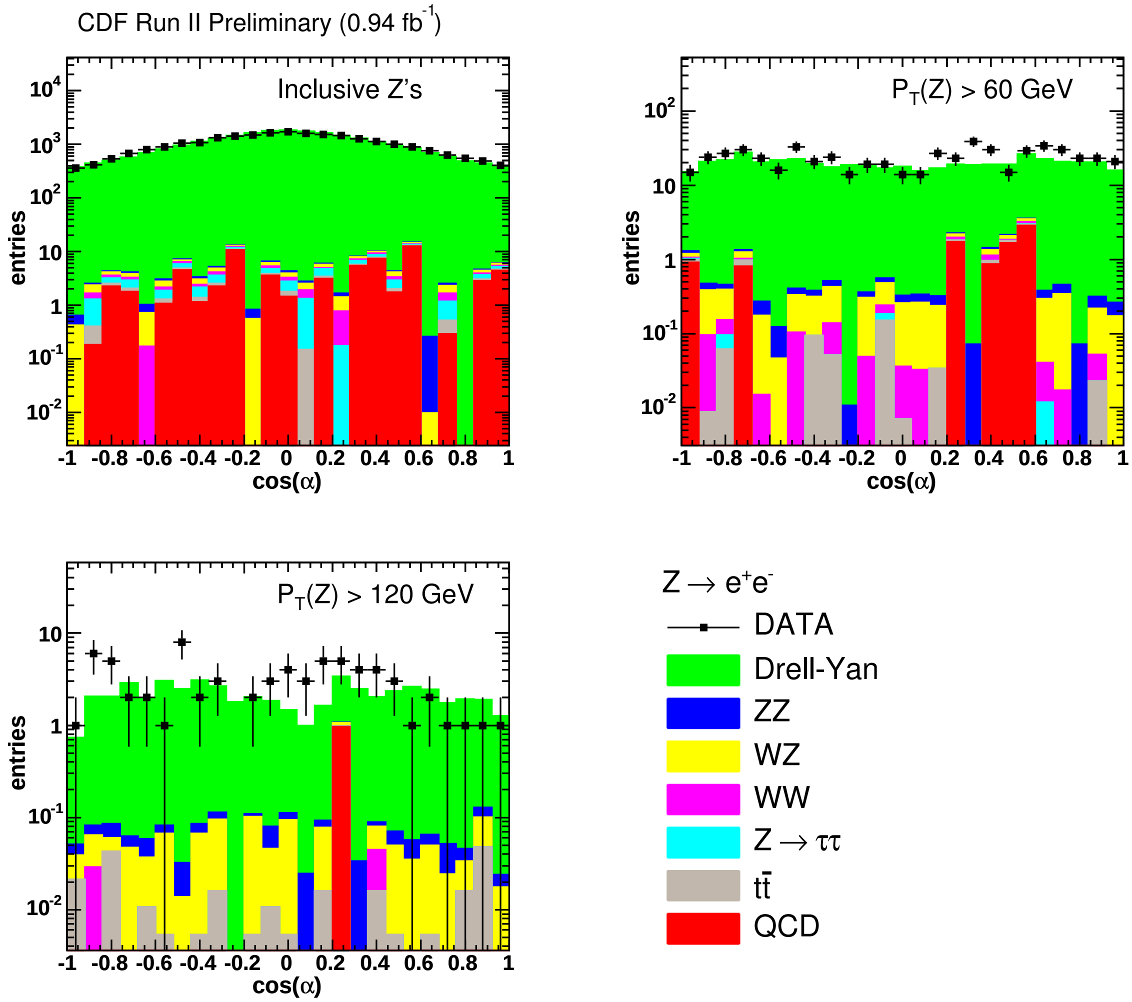

Figure 9: The distribution of $cos(\alpha)$ is shown for the subsamples of $Z \to ee$ with $P_T(Z)$ cuts ($>$ 0 GeV, $>$ 60 GeV, and $>$ 120 GeV). The mass cut of 66 $<$ M(ee) $<$ 116 GeV has been applied.

[5] +1 773 957 3694

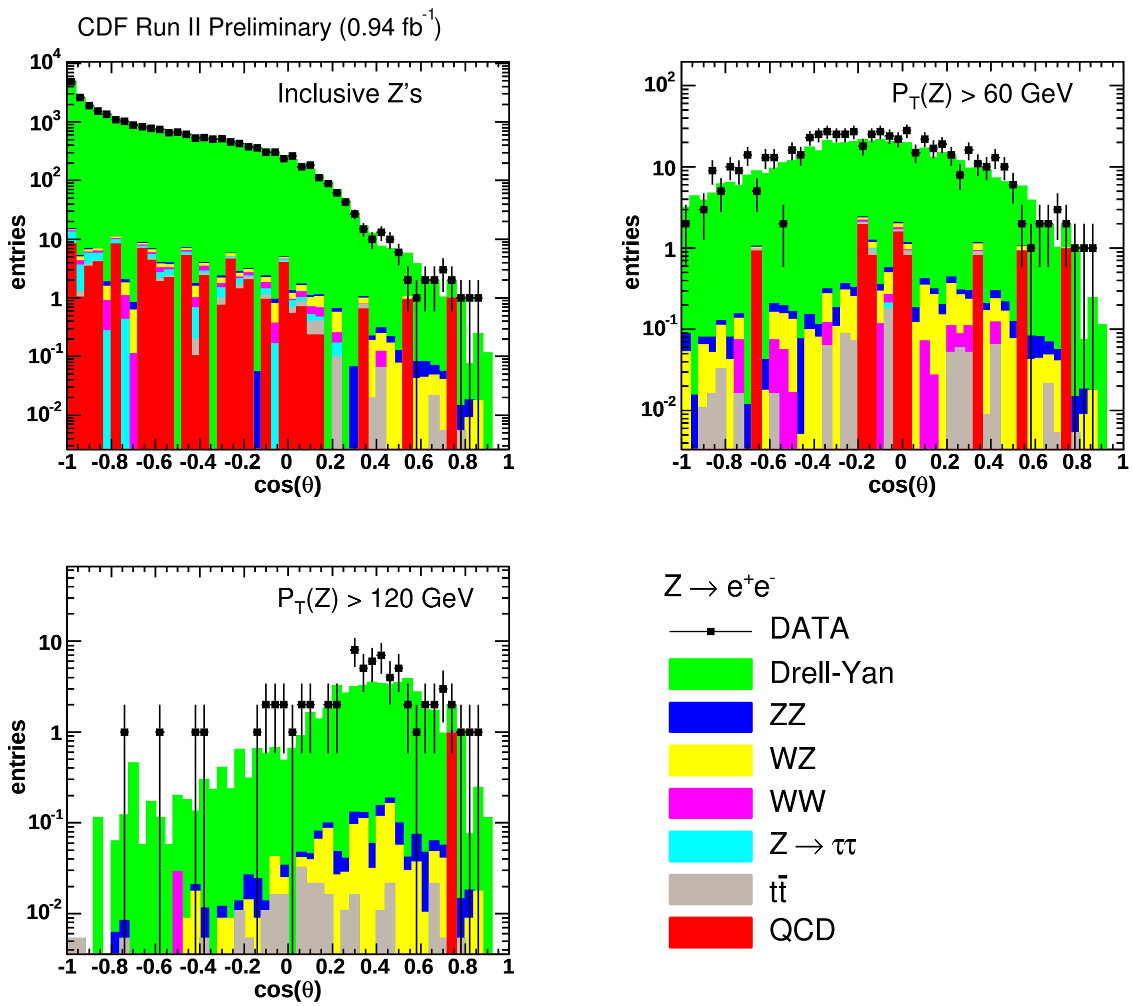

Figure 10: $cos(\theta)$ denotes the angle between e^+ and e^- in the rest frame of the CDF. The distributions are made for $Z \to ee$ with different cuts on $P_T(Z)$.

6.2 $Z \to \mu\mu$ sample.

We repeat the plots of the previous section as for the $Z \to ee$.

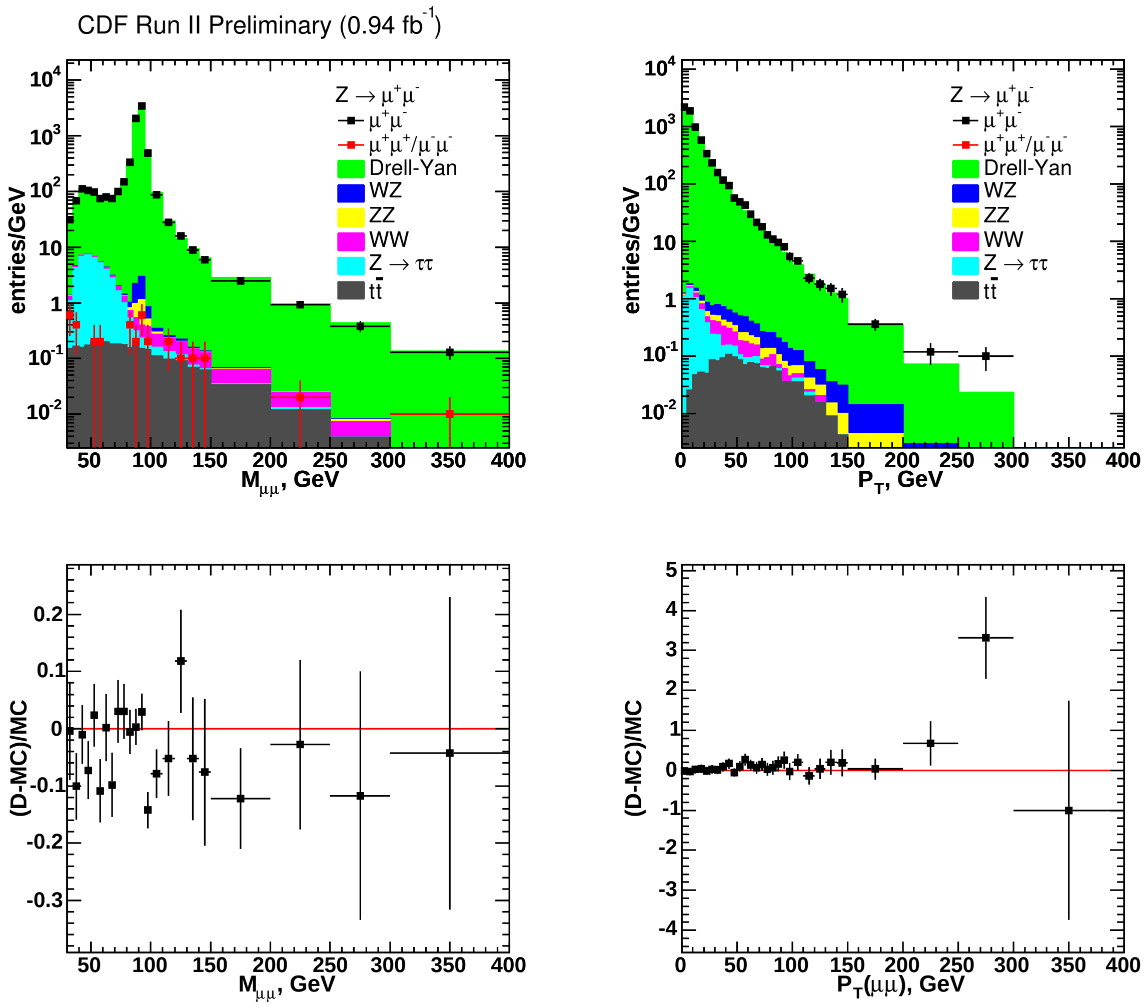

Figure 11: Invariant mass (left) and transverse momentum (right) for $Z \to \mu\mu$. The two lower plots show the difference between the numbers of expected and observed events divided by the number expected. A mass cut of $66 < \mathrm{M}(\mu\mu) < 116$ GeV has been applied to the right-hand plot.

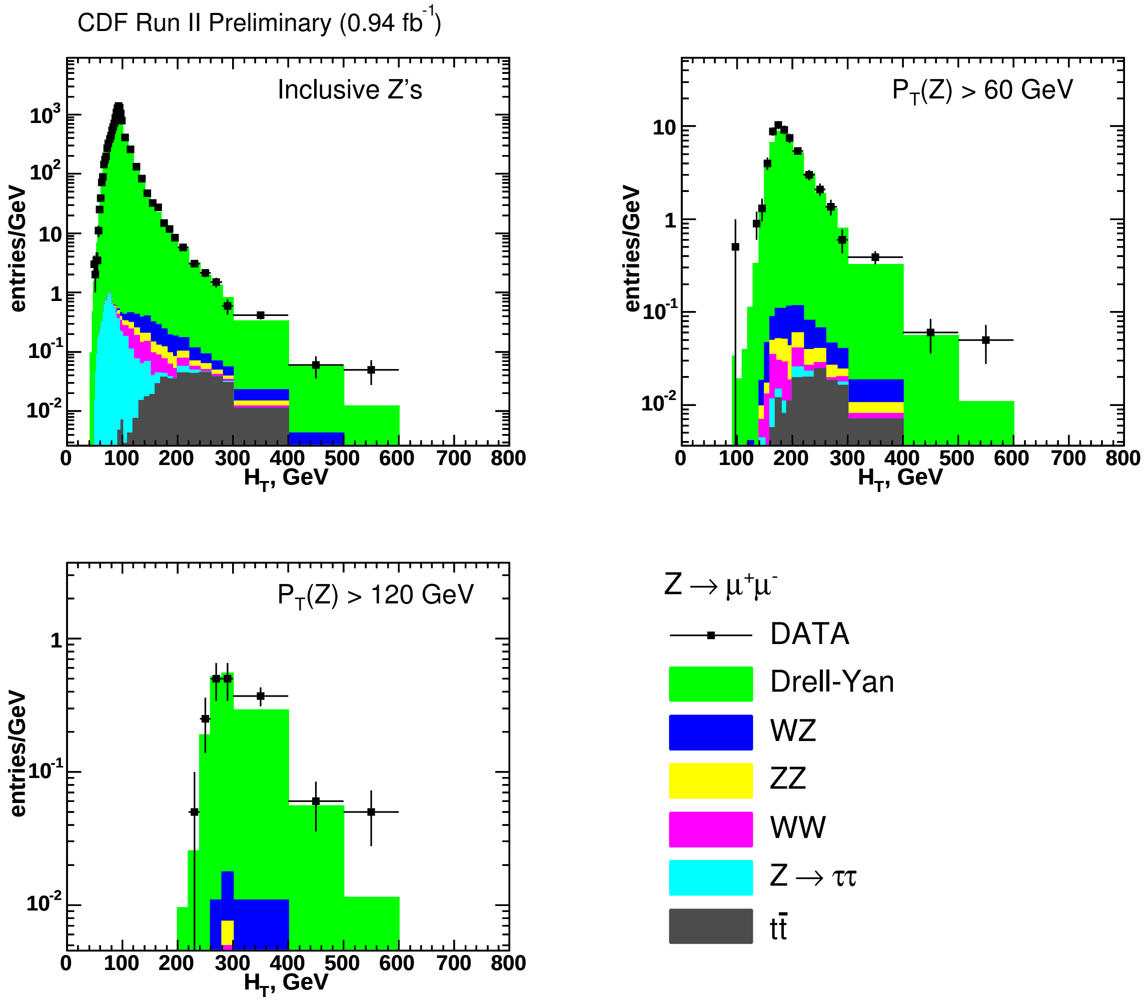

Figure 12: A comparison of H_T (scalar sum of E_T over all objects in an event)for the $Z \to \mu\mu$ data and SM MC. The distributions are calculated for three subsamples of $Z \to \mu\mu$ with different cuts on $P_T(Z) >$: 0 GeV, 60 GeV, and 120 GeV. The mass cut of 66 < M($\mu\mu$) < 116 GeV has been applied.

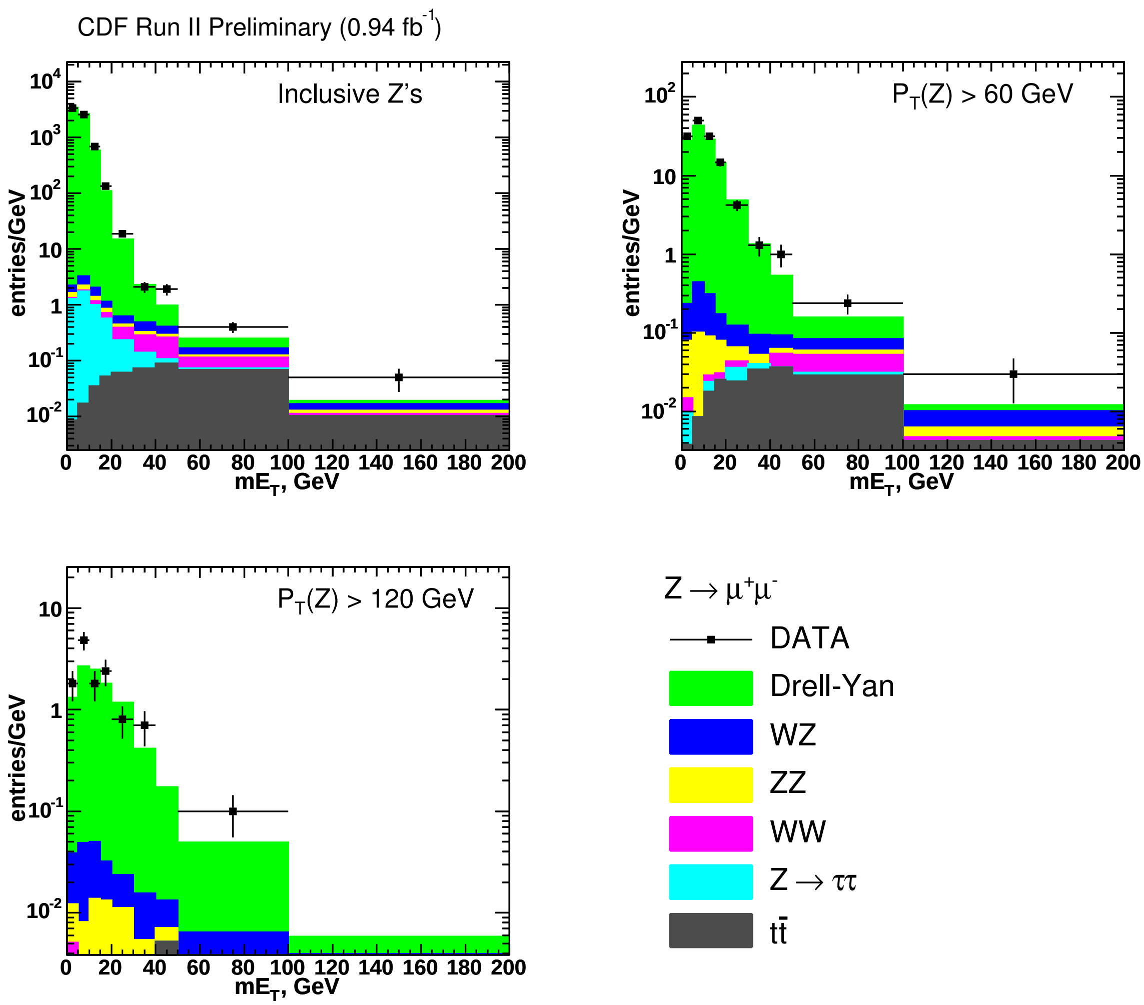

Figure 13: The measured distributions for $\not\!\!E_T$ are compared to SM expectations for three subsamples of $Z \rightarrow \mu\mu$ with different cuts on $P_T(Z) >$: 0 GeV, 60 GeV, and 120 GeV. The mass cut of $66 < \mathrm{M}(\mu\mu) < 116$ GeV has been applied.

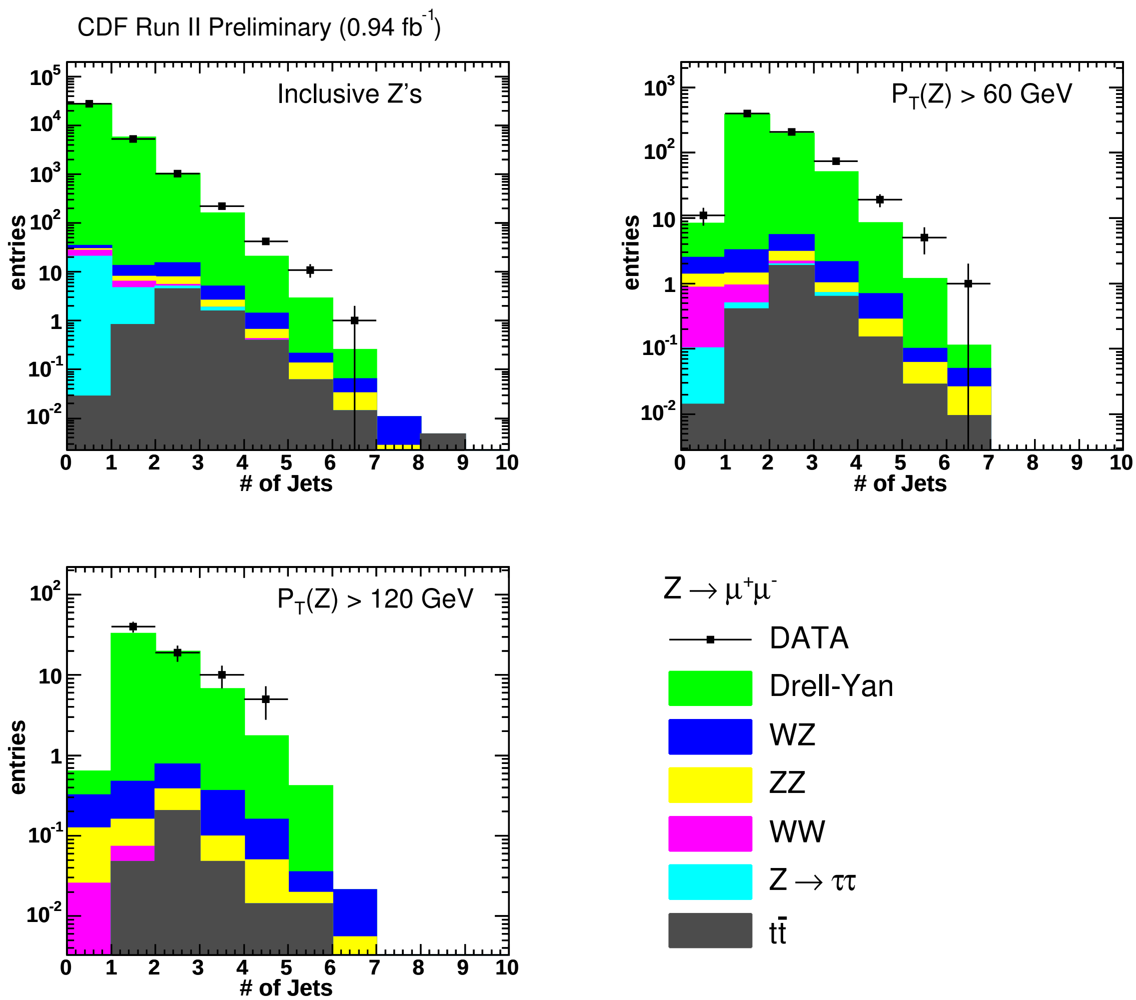

Figure 14: The measured distributions for the number of jets in data compared to SM expectation for the subsamples of $Z \to \mu\mu$ with $P_T(Z)$ cuts (> 0 GeV, > 60 GeV, and > 120 GeV). The mass cut of $66 < \mathrm{M}(\mu\mu) < 116$ GeV has been applied.

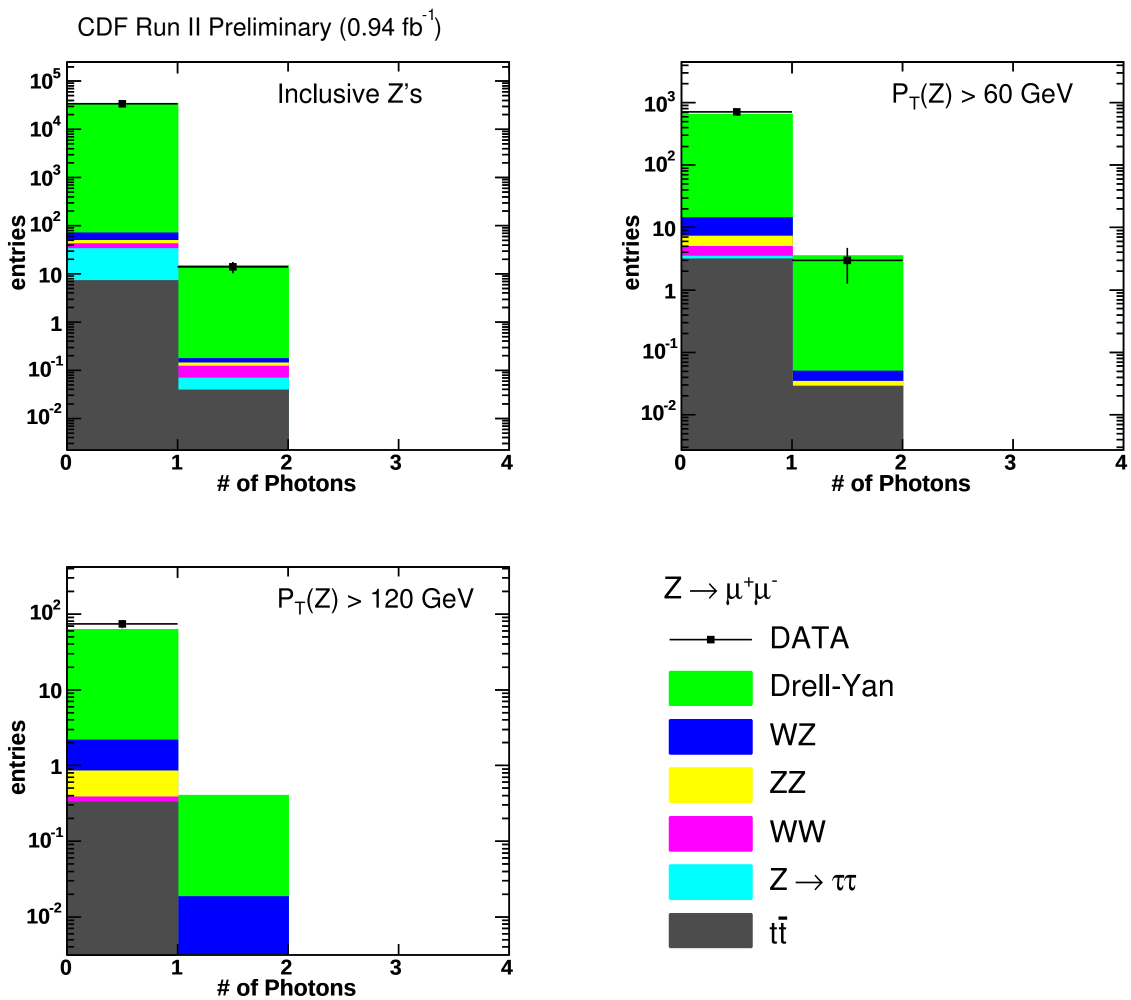

Figure 15: The measured distributions for the numbers of photons in data compared to SM expectations for $Z \to \mu\mu$ subsamples $P_T(Z)$ cuts (> 0 GeV, > 60 GeV, and > 120 GeV). The mass cut of $66 <$ M$(\mu\mu) < 116$ GeV has been applied.

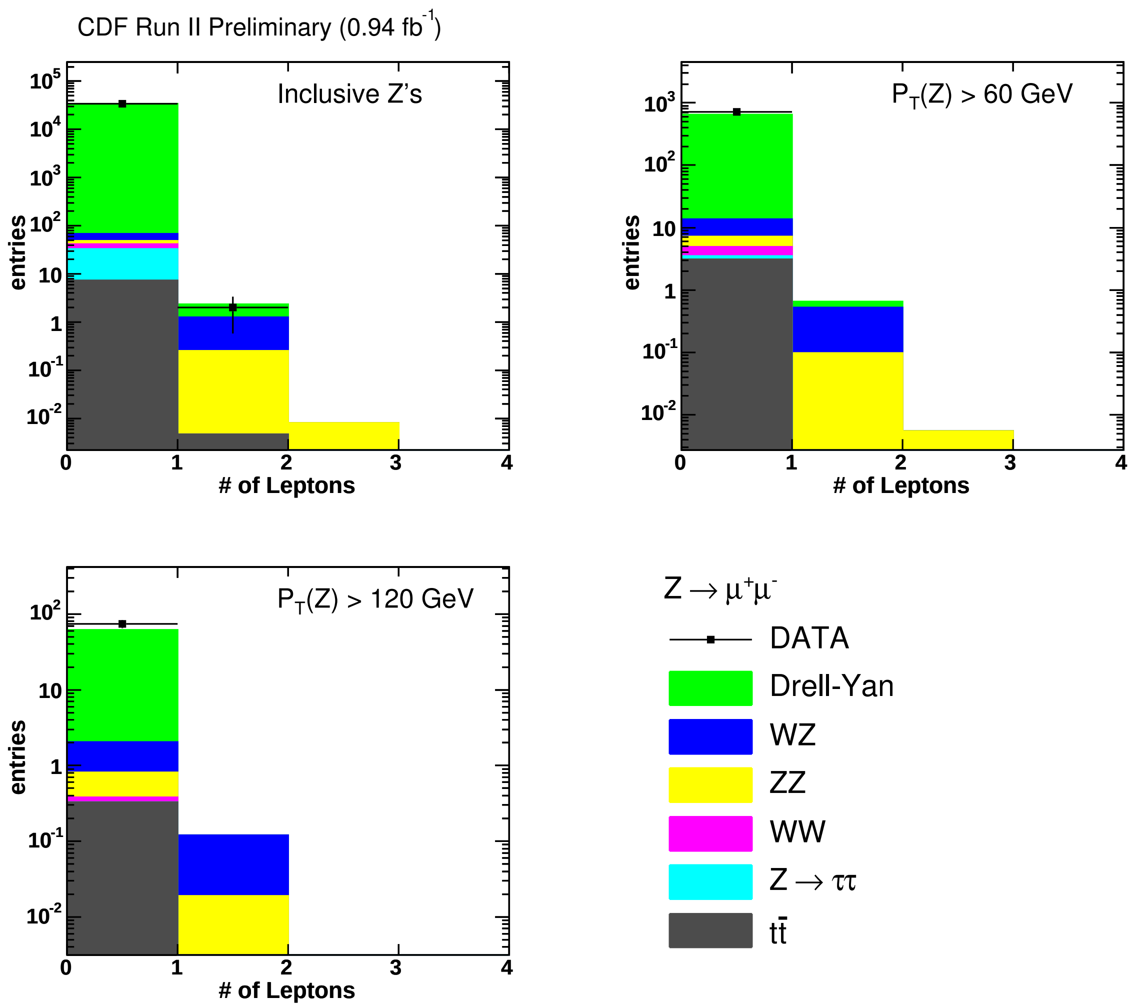

Figure 16: The measured distributions for the number of leptons in data compared to the SM expectations for the $Z \to \mu\mu$ samples with different $P_T(Z)$ cuts. The mass cut of $66 < \mathrm{M}(\mu\mu) < 116$ GeV has been applied.

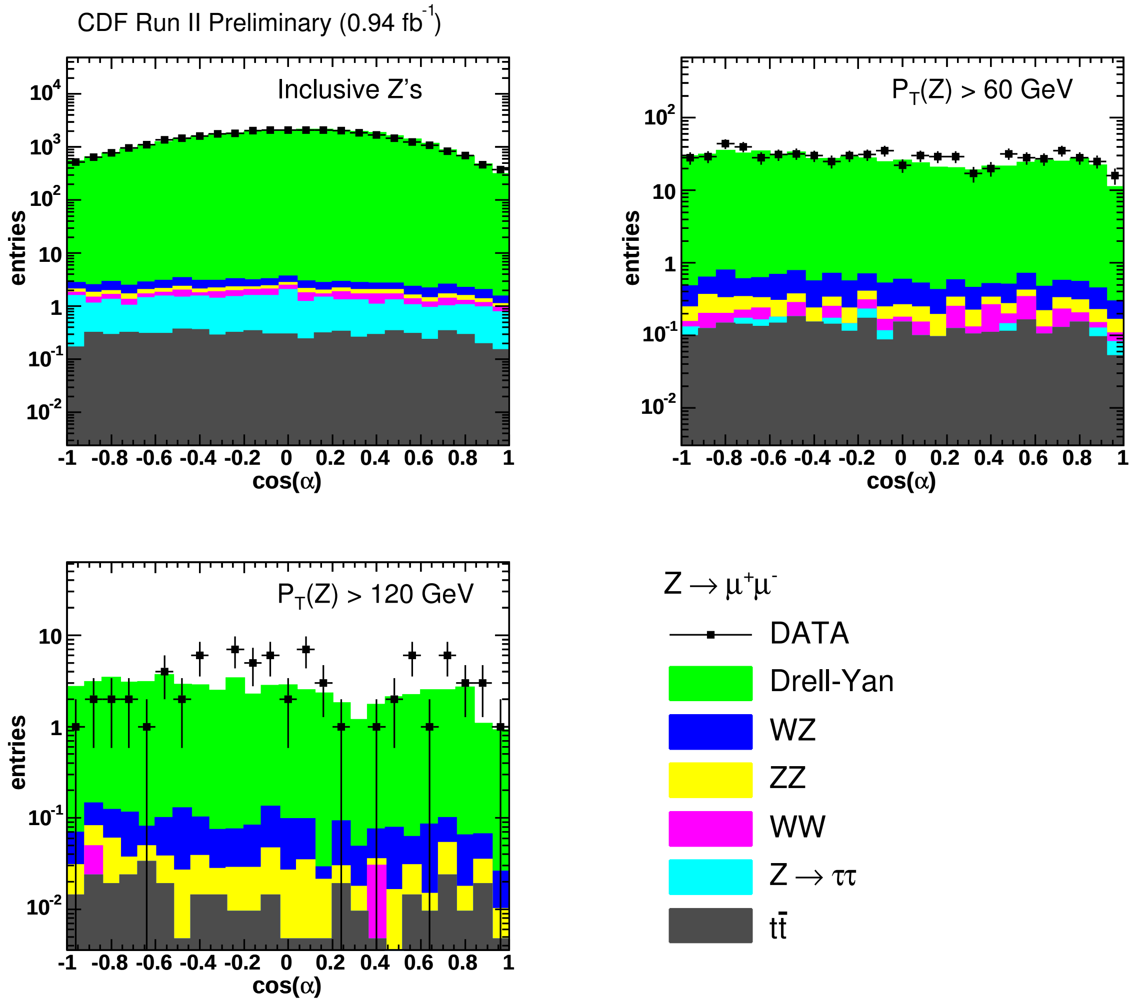

Figure 17: $cos(\alpha)$ (angle between $\vec{P}(Z)$ and positively charged lepton in the rest frame of Z^0) is for subsamples of $Z \to \mu\mu$ with $P_T(Z)$ cuts (> 0 GeV, > 60 GeV, and > 120 GeV).

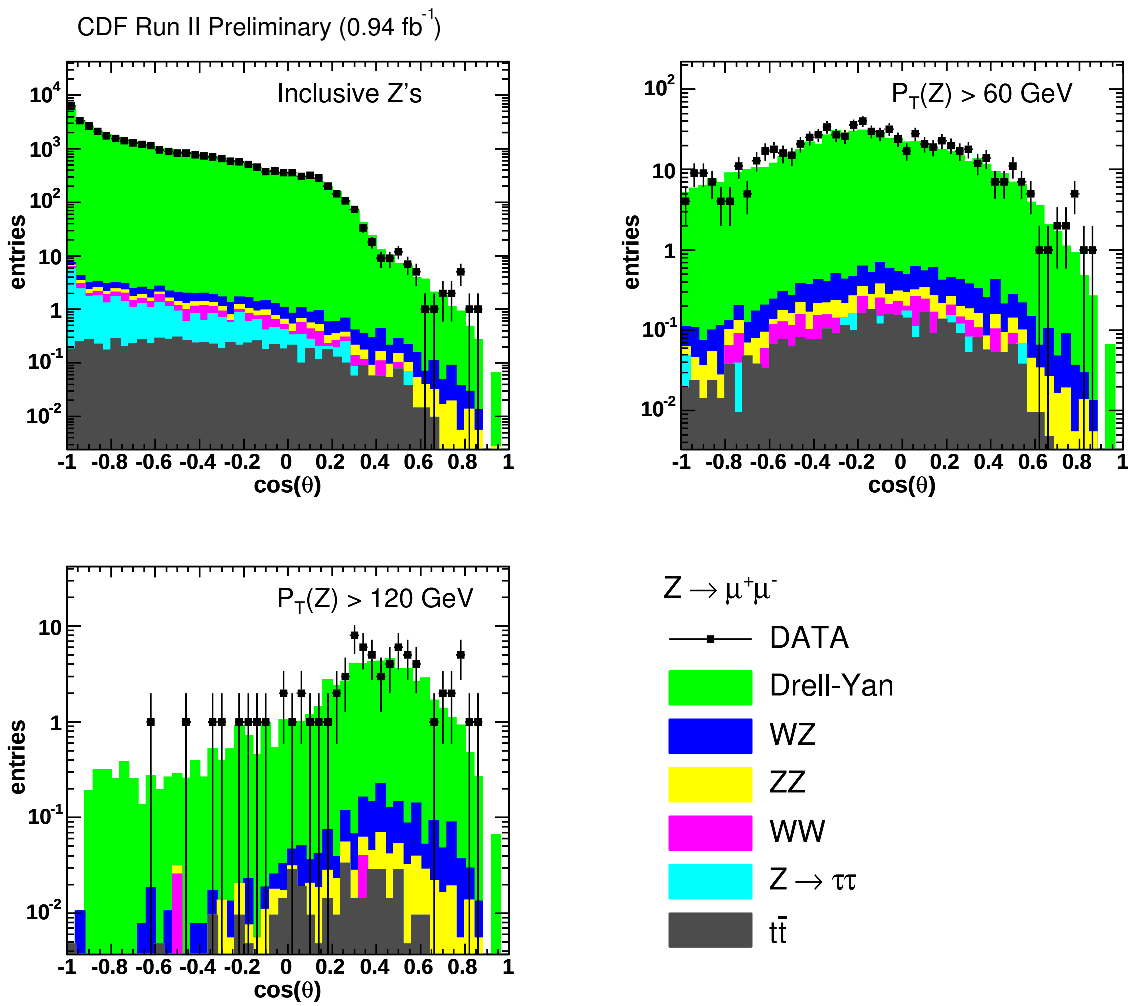

Figure 18: $cos(\theta)$ denotes the angle between e^+ and e^- in the rest frame of the CDF. The distributions are made for $Z \to \mu\mu$ with different cuts on $P_T(Z)$.

6.3 Stability plots for $Z \to ee$ and $Z \to \mu\mu$

We split the data into sections which correspond to different trigger tables and running periods of CDF. This lets us study the stability of the detector performance. We calculate the ratio of the number of reconstructed Z-bosons in each sample to the observed luminosity of the sample. The figures for inclusive $Z \to ee$ and $Z \to \mu\mu$ events are shown in Fig. 19. It's not as stable as it should be, but it seems to be good enough for CDF.

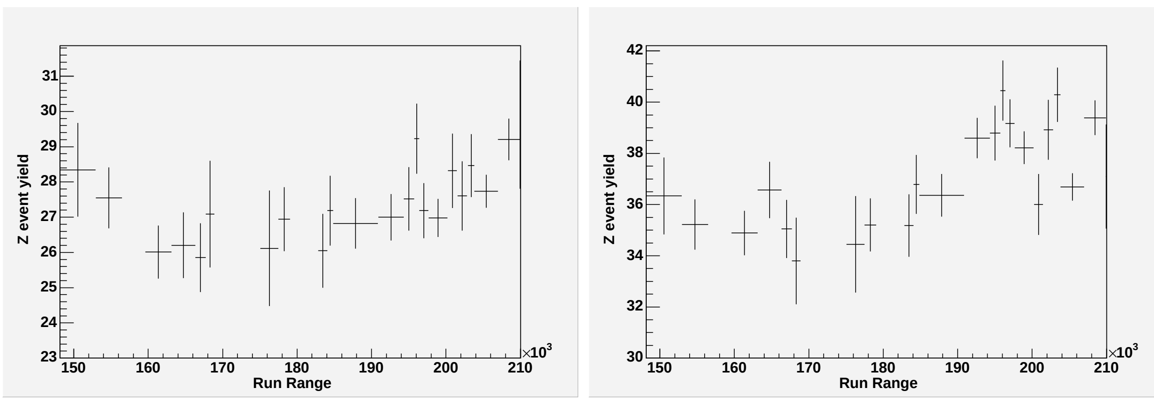

Figure 19: Yield per pb^{-1} for $Z \to \mu\mu$ (right) and $Z \to ee$ (left) modes.

Please take into account that the yield in $Z \to \mu\mu$ mode is higher than the $Z \to ee$ one because of our reconstruction procedure. The reconstruction of $Z \to ee$ takes two CEM clusters ($|\eta| < 1$ of each cluster). However, the $Z \to \mu\mu$ decay is reconstructed using a tight muon (which has a CMUP or CMX stub) and a loose muon (a good isolated track). The $|\eta|$ range of the track is much bigger that the one of a tight muon or a CEM electron. This improves the acceptance of $Z \to \mu\mu$ decays as you can see above.

7 High Pt Signal Region: Comparison of the SM MC and Data

The distributions of $P_T(Z)$ for $Z \to ee$ and $Z \to \mu\mu$ are in a good agreement with SM (PYTHIA) predictions (see figures 3 and 11). The distributions of the ratios of the data to MC differences relative to the MC include the systematic uncertainties on the SM predictions of the $P_T(Z)$ distribution. The sources of the systematic uncertainty are discussed below in the next section.

8 Systematic Uncertainties

8.1 Theoretical uncertainties on the shape of $P_T(Z)$ distribution

There are four sources of theoretical uncertainty:

- the choice of renormalization scale that minimizes higher-order corrections,
- the value of Λ_{QCD},
- the parametrization of the structure functions,
- resummation at low P_T.

The error of 10% is taken for the entire range of $P_T(Z)$ (See [13] for more details). Prediction of the PYTHIA MC were compared with NNLO ResBos (CTEQ4M) in [14] and found in a good agreement.

8.2 Uncertainties on acceptance and reconstruction efficiency

The systematic uncertainties on efficiency and acceptance are studied in [15], where the same selection criteria were used. The summary of the systematic uncertainties are given in the tables 8 and 9. The uncertainty due to statistics of the simulated events is included separately.

Uncertainty Type	$\Delta A(Z \to ee)$	$\Delta A(Z \to \mu\mu)$
NNLO $d\sigma/dy$ Calculation	0.06%	0.72%
PDF Model (positive)	0.69%	1.72%
PDF Model (negative)	0.84%	2.26 %
Boson P_T model	0.06%	0.08%
Track P_T Scale/Resolution	0.04%	0.05%
Cluster E_T Scale/Resolution	0.26%	0.00%
Detector Material Model	0.96%	0.00%
Total (positive)	1.21%	1.87%
Total (negative)	1.30%	2.37%

Table 8: Acceptance uncertainty summary. (From Ref. [15])

Sample	Uncertainty
$Z \to ee$	1.68%
$Z \to \mu\mu$	2.10%

Table 9: Efficiency uncertainty summary. (From Ref. [15])

The error on the luminosity is taken to be 6%, which is dominated by the uncertainty in absolute normalization of the CLC acceptance for a single $p\bar{p}$ inelastic collision.

9 Acceptance and Efficiency.

The acceptance and efficiency ratios are taken from the MC predictions. The numbers of Z's are counted before applying any cuts and after reconstruction. The ratio is P_T -dependent and calculated for the same bins as the distribution of $P_T(Z)$ (see Fig. 20).

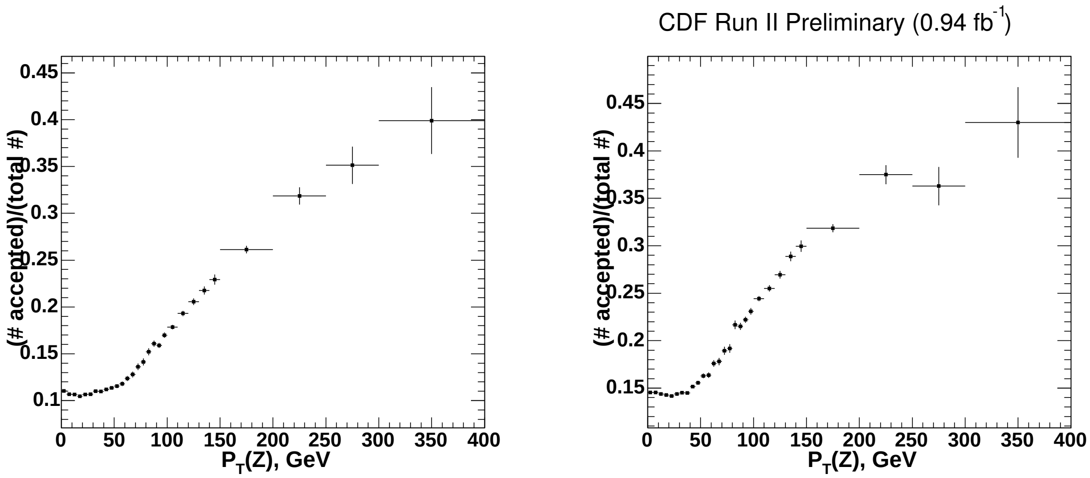

Figure 20: Acceptance*Efficiency for $Z \to \mu\mu$ (right) and $Z \to ee$ (left) modes. The uncertainties (error bars) are due to limited statistics of the MC samples. The systematical uncertainties will be taken into account later.

10 Statistical Agreement in high-P_T region

We use a Bayesian approach to calculate an upper limit on a cross section in the presence of uncertainties on background level and acceptance. The limit calculation software is implemented in a package (see [16]) presented by the CDF Statistics Committee (see [17]). The more complete description of the approach can be found in [18].

Summarizing briefly the situation, we observe N events, which includes both signal and background. The observed events are used to set an upper limit σ_u on the cross section σ at confidence level β (we take $\beta = 0.95$). The upper limit includes the expected background $b \pm \sigma(b)$ and efficiency $\epsilon \pm \sigma(\epsilon)$, which includes reconstruction efficiency and acceptance. The n observed events are considered to be a deviation from a Poisson distribution having a mean of $(\sigma * L * \epsilon + b)$, where L is the observed luminosity.

$$\int_0^{\sigma_u} p(\sigma|N) d\sigma = \beta \tag{8}$$

The prior p.d.f. for σ is chosen to be $\sigma^{\alpha-1}d\sigma$, where α =0.5 (normally $0.5 \geq \alpha \geq 1$).

11 Results: Limits on anomalous production of the inclusive Z-bosons

The Bayesian approach (see Sect. 10) is applied bin-by-bin to the distribution of $P_T(Z)$ for $Z \to ee$ and $Z \to \mu\mu$ separately. The cross section limits obtained are presented in Figures 21 and 22 for $Z \to ee$ and $Z \to \mu\mu$ respectively. The corresponding cumulative (integral) Bayesian limits are shown in Fig. 24. We assume that the production mechanism is the same as for the Standard Model.

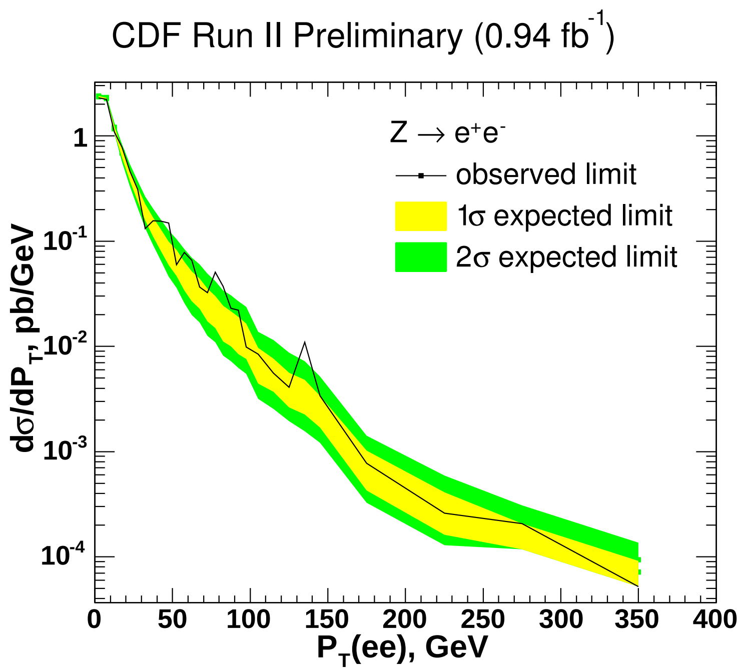

Figure 21: The Bayesian limit on the differential cross section for anomalous $Z \to ee$ production at 95% CL. The yellow band represents the expected limit for 1σ fluctuations of the observed events in each bin, the green band - 2σ.

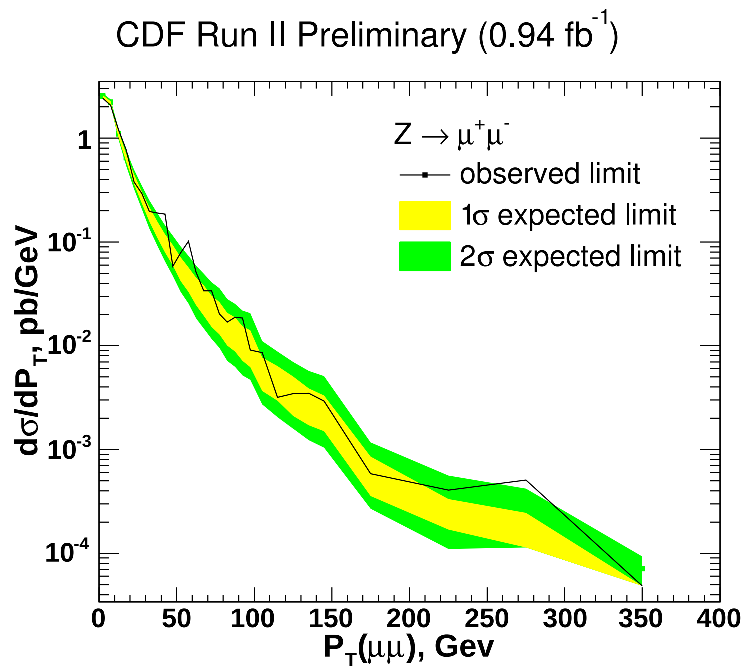

Figure 22: The Bayesian limit on the differential cross section for anomalous $Z \to \mu\mu$ production at 95% CL. The yellow band represents the expected limit for 1σ fluctuations of the observed events in each bin, the green band - 2σ.

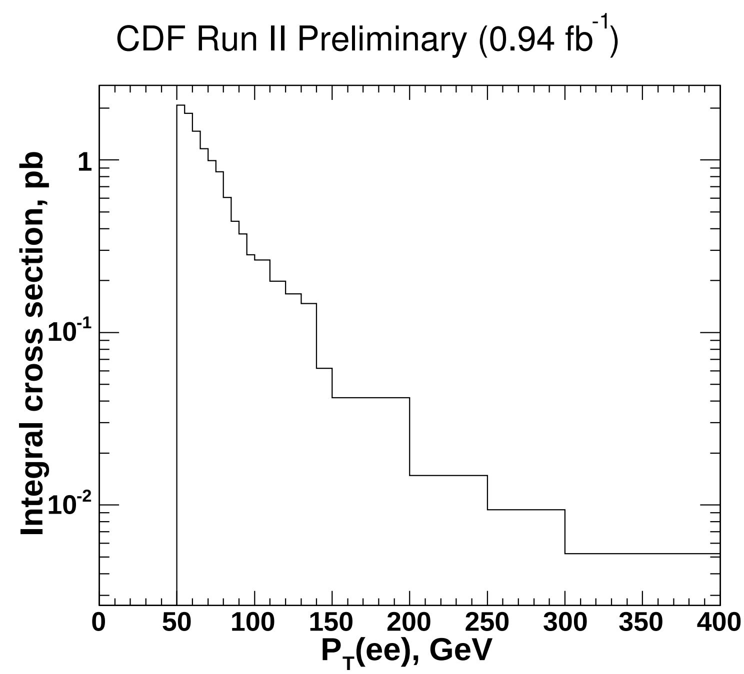

Figure 23: Bayesian limit on the integral cross sections of anomalous production in $Z \to ee$ mode. The limit is set at 95% CL.

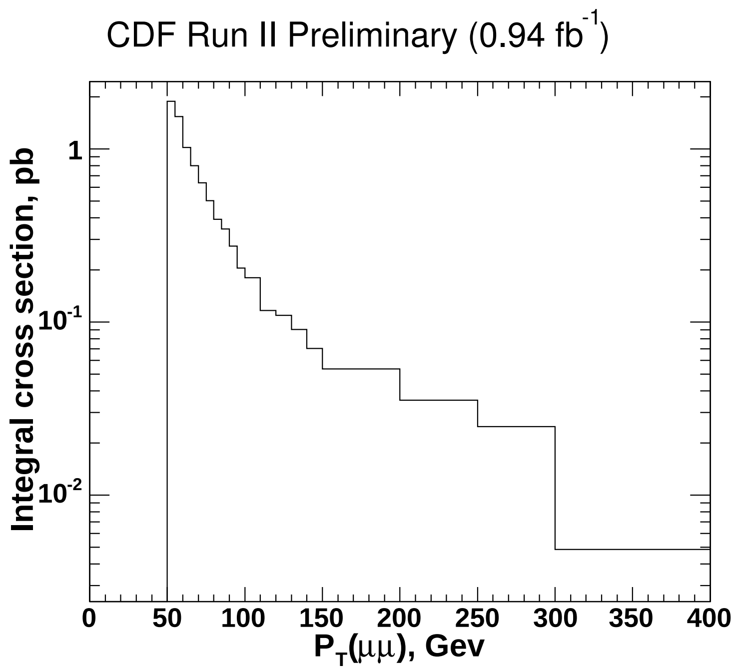

Figure 24: Bayesian limit on the integral cross sections of anomalous production in $Z \to \mu\mu$ mode. The limit is set at 95% CL.

12 Z+X signatures

In order to make the search for new physics sensitive to smaller cross-sections, we have added additional signatures to the high-Pt Z signature starting point. This reduces the SM backgrounds in a given category, although it necessarily narrows the search. In this section we consider a high-Pt Z plus one additional object, 'X', where X can be additional leptons, photons, signature of missing transverse energy ($\not\!\!E_T$), or large transverse energy (H_T). We step through these in turn below.

12.1 Z+X, $Z \to ee$

The p_T spectrum of the Z boson in events with at least one additional tight central lepton (e or μ) with $E_T > 20$ GeV is shown in Figure 25. The spectrum is dominated by Z+N jets, where a jet fakes a lepton, although there are contributions from SM WZ and ZZ production.

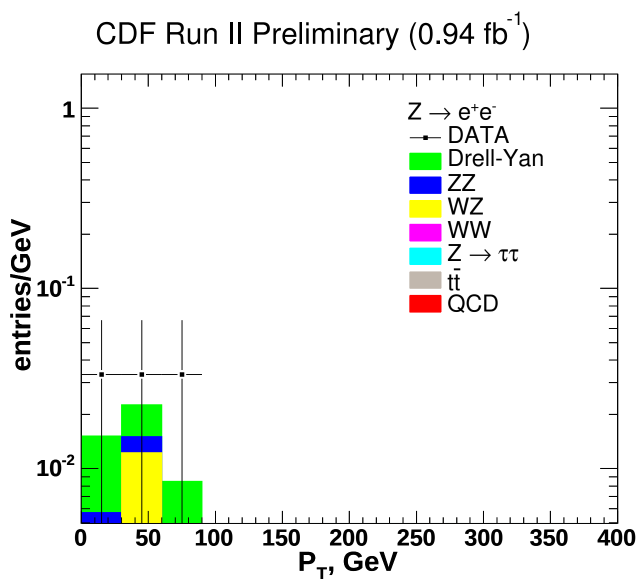

Figure 25: The measured distributions for "Z + Leptons" in data compared to SM expectation The mass cut of $66 < M(ee) < 116$ GeV has been applied.

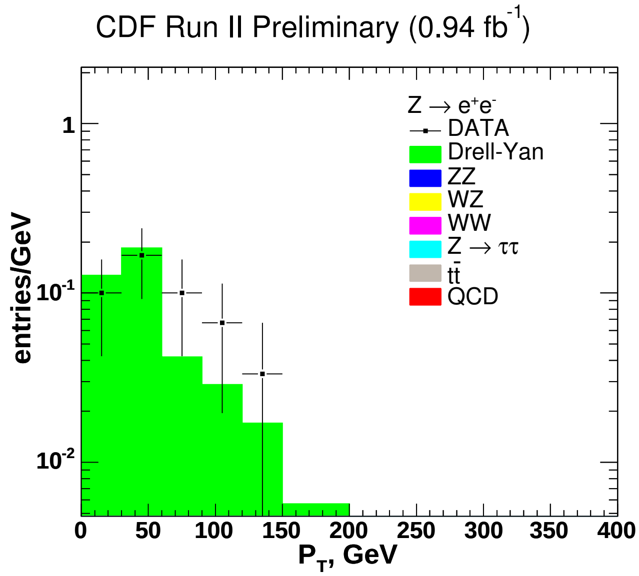

Figure 26: The measured distributions for "Z + Photons" in data compared to SM expectation The mass cut of 66 < M(ee) < 116 GeV has been applied.

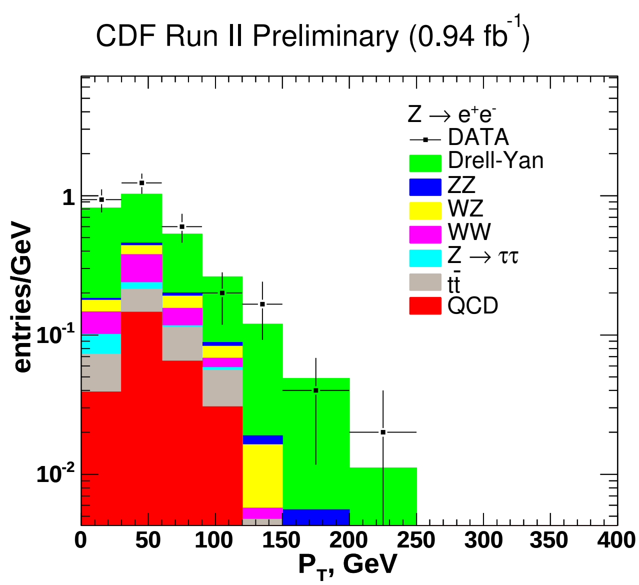

Figure 27: The measured distributions for "Z + $\not{E}_T$-signature" in data compared to SM expectation The mass cut of 66 < M(ee) < 116 GeV has been applied.

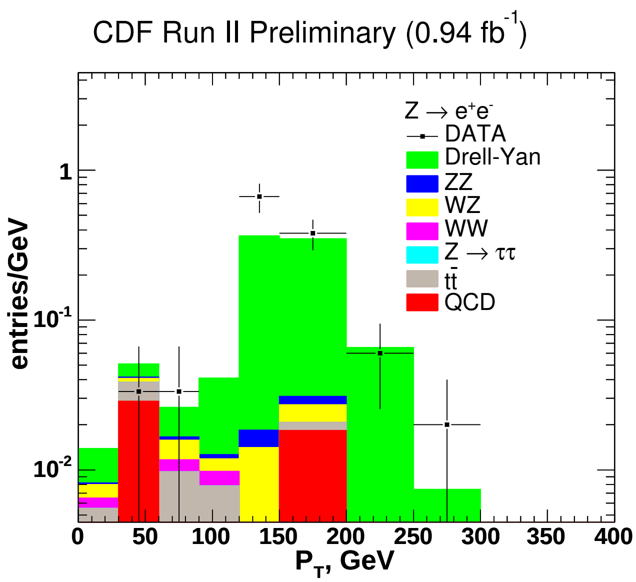

Figure 28: The measured distributions for "Z + H_T (H_T > 300 GeV)" in data compared to SM expectation The mass cut of 66 < M(ee) < 116 GeV has been applied.

12.2 Z+X, $Z \to \mu\mu$

No we repeat the same plots as in the previous section but for $Z \to \mu\mu$ decay mode.

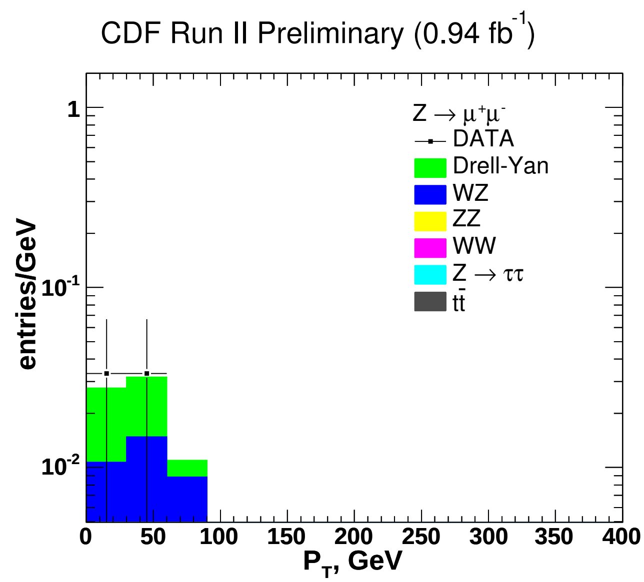

Figure 29: The measured distributions for "Z + Leptons" in data compared to SM.

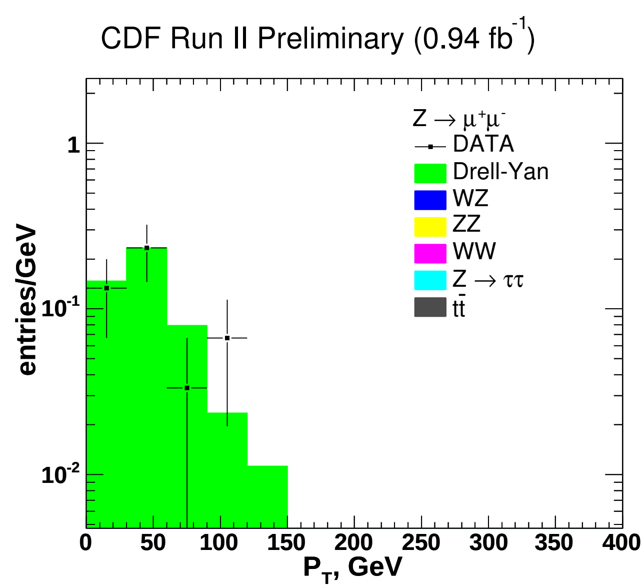

Figure 30: The measured distributions for "Z + Photons" in data compared to SM expectation The mass cut of 66 < M($\mu\mu$) < 116 GeV has been applied.

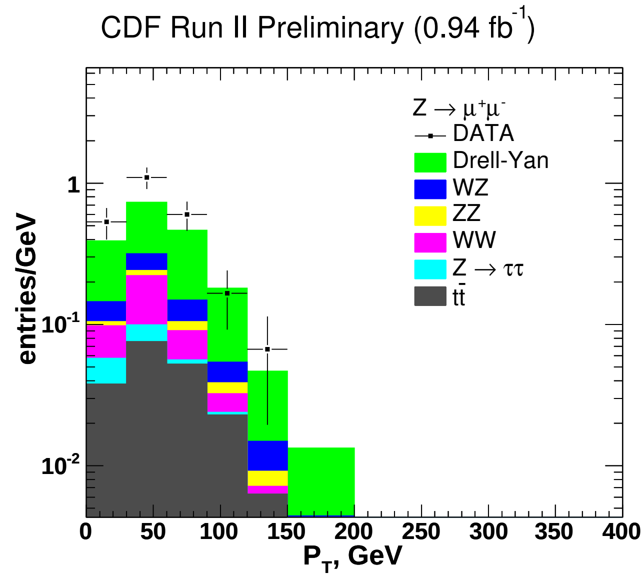

Figure 31: The measured distributions for "Z + $\not\!\!E_T$-signature" in data compared to SM expectation The mass cut of 66 < M($\mu\mu$) < 116 GeV has been applied.

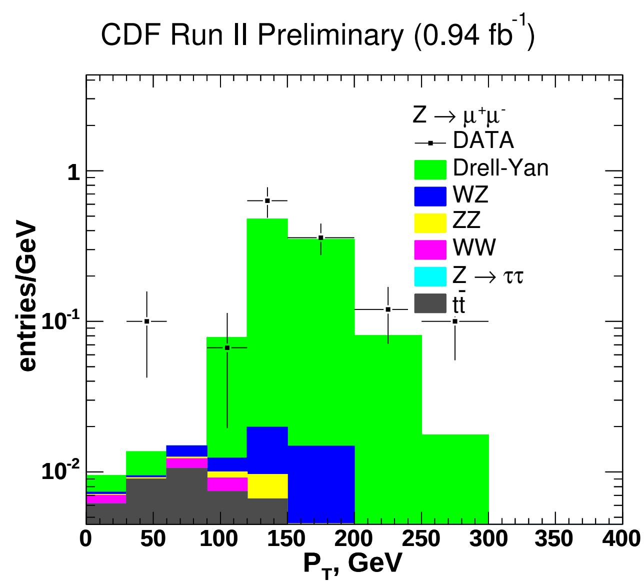

Figure 32: The measured distributions for "Z + H_T" (H_T > 300 GeV) in data compared to SM expectation

13 Z+X+Y signatures

The new physics we are looking for in events with high-Pt Z bosons would involve the decays of one or a pair of new heavy objects. It is not unreasonable that there would be multiple additional objects beyond the high-Pt Z in such events. For example, in the model of Bjorken, Pakvasa, and Tuan [19], heavy right-handed new quarks would be produced with strong cross-sections, and each would decay to a light quark plus a heavy boson (W, Z, or H), giving several signatures with a high-Pt Z plus multiple objects). The SM background to high-Pt Z's is largely QCD production of Z + jets. Thus a search for high-Pt Z+ two or more additional objects, where the additional objects can be leptons, photons, missing Et or high Ht, could be sensitive to smaller cross-sections. In this section we consider a high-Pt Z plus two additional objects, 'X' and 'Y', where X or Y can be additional leptons, photons, signature of missing transverse energy ($\not{E}_{\mathrm{T}}$), or large transverse energy (H_T). We step through their combinations in turn below.

13.1 Z+X+Y, $Z \to ee$

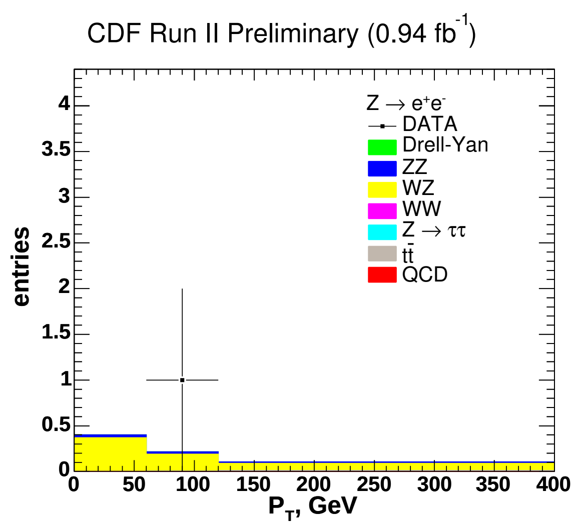

Figure 33: The measured distributions for "Z + Lepton + $\not{E}_{\mathrm{T}}$-signature" in data compared to SM expectation The mass cut of 66 < M($\mu\mu$) < 116 GeV has been applied.

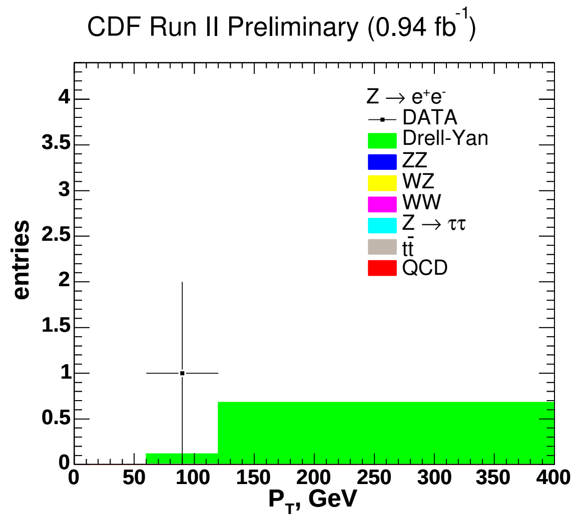

Figure 34: The measured distributions for "Z + Photon + H_T > 300 GeV." in data compared to SM expectation The mass cut of 66 < M($\mu\mu$) < 116 GeV has been applied.

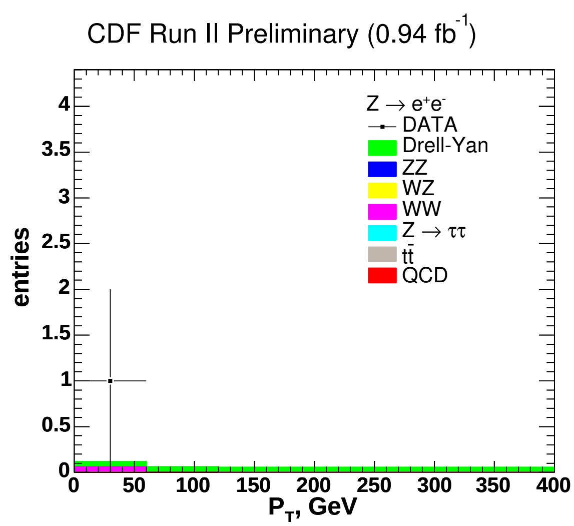

Figure 35: The measured distributions for "Z + Photon + $\not\!\!E_T$-signature" in data compared to SM expectation The mass cut of 66 < M($\mu\mu$) < 116 GeV has been applied.

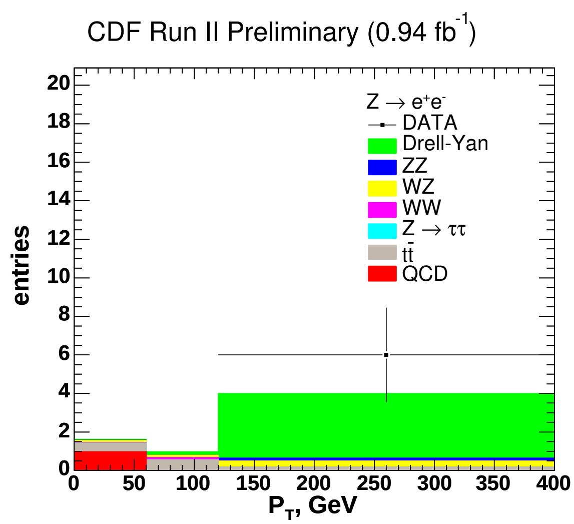

Figure 36: The measured distributions for "Z + H_T + $\not{E}_T$-signatures" in data compared to SM expectation The mass cut of 66 < M($\mu\mu$) < 116 GeV has been applied.

13.2 Z+X+Y, $Z \rightarrow \mu\mu$

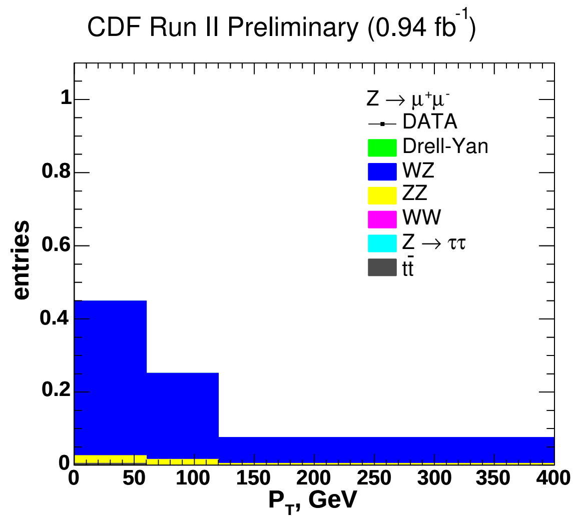

Figure 37: The measured distributions for "Z + Lepton + $\not\!\!E_{\mathrm{T}}$-signature" in data compared to SM expectation The mass cut of 66 < M($\mu\mu$) < 116 GeV has been applied.

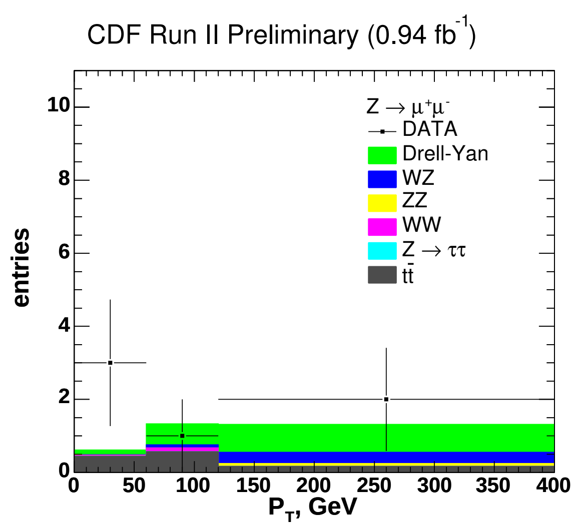

Figure 38: The measured distributions for "Z + H_T + $\not\!\!E_{\mathrm{T}}$-signature" in data compared to SM expectation The mass cut of 66 < M($\mu\mu$) < 116 GeV has been applied.

14 Summary tables of the Z+X and Z+X+Y signatures.

We summarize the Z+X and Z+X+Y search by presenting two tables of events observed in each category of X and Y. We do this separately for $Z \to ee$ and $Z \to \mu\mu$ processes. The tables can be found below. The uncertainties on the expected numbers of events are systematical. The systematical uncertainties due to jet energy corrections are taken into account.

	Leptons	Photons	$H_T > 300$ GeV	$\not{E}_\mathrm{T}$-signature
Leptons	3 / 1.6 ± 0.3	0 / 0.01 ± 0.01	0 / 0.16 ± 0.04	1 / 0.72 ± 0.11(WZ)
Photons	-	14 / 12.4 ± 1.5	1 / 0.80 $^{+0.34}_{-0.23}$	1 / 0.24 ± 0.20
H_T	-	-	45 / 36.4 $^{+4.9}_{-5.8}$	6 / 6.6 ± 1.0
$\not{E}_\mathrm{T}$-sign.	-	-	-	97 / 85.4 ± 12.3

Table 10: Numbers of (observed / expected) events are listed for each category of Z+X+Y, $Z \to ee$. "X" corresponds to the objects listed in the rows and "Y" - in the columns. The diagonal elements of the table represent Z+X categories.

	Leptons	Photons	$H_T > 300$ GeV	$\not{E}_\mathrm{T}$-signature
Leptons	2 / 2.4 ± 0.4	0 / 0.01 ± 0.01	0 / 0.14 $^{+0.05}_{-0.04}$	0 / 0.8 ± 0.1 (WZ)
Photons	-	14 / 15.0 ± 1.8	0 / 0.28 $^{+0.14}_{-0.13}$	0 / 0.19 $^{+0.21}_{-0.10}$
H_T	-	-	53 / 41.3 $^{+5.0}_{-5.2}$	6 / 3.5 ± 0.5
$\not{E}_\mathrm{T}$-sign.	-	-	-	74 / 55.9 $^{+9.7}_{-5.8}$

Table 11: Numbers of (observed / expected) events are listed for each category of Z+X+Y, $Z \to \mu\mu$. "X" corresponds to the objects listed in the rows and "Y" - in the columns. The diagonal elements of the table represent Z+X categories.

15 Conclusions

We have repeated our previous analysis (CDF8033) with additional signatures associated with the Z-production. Basically, we observe the same good agreement between the data as before and the SM predictions of the inclusive production of the Z-bosons. This comparison works as a control region in this analysis. Also we calculate limits on differential cross sections for anomalously produced Z-bosons assuming that the anomalous production has the SM acceptance and efficiency. These limits correspond to processes where the Z-bosons are produced with high transverse momenta.

In addition to the existing study we also analyzed production of Z bosons associated with one or two additional signatures, i.e. 'Z+X+anything' and 'Z+X+Y+anything'.

The idea of using signatures is to get to regions where the SM Z-production is small and the new physical processes could be observed more easily. For example, we do observe WZ production in the 'Z + Leptons + Missing Energy' category.

These X and Y can be the signatures of extra leptons, photons, missing energy, or high transverse energy. Therefore we have 10 categories:

1. Z + Leptons
2. Z + Photons
3. Z + Missing Energy
4. Z + High Transverse Energy
5. Z + Leptons + Missing Energy
6. Z + Leptons + Photons
7. Z + Leptons + High Transverse Energy
8. Z + Photons + Missing Energy
9. Z + Photons + High Transverse Energy
10. Z + Missing Energy + High Transverse Energy

The number of events in each category was compared to the SM predictions and they agree within uncertainties. Distributions of transverse momenta of the Z-bosons are in agreement with the predictions too. We are bored by this...

16 Acknowledgments

We are grateful to Stephen Levy, Collin Wolfe, Carla Pilcher, Alexei Safonov, Song Ming Wang, and Giulia Manca for a number of very helpful discussions.

References

[1] D. Toback. *Searches for New Physics in Diphoton Events in $\bar{p}p$ Collisions at $\sqrt{s}$ =1.8 TeV.* PhD thesis, University of Chicago, December 1997.

[2] J. Berryhill. *Searches for New Physics in Photon-Lepton Events in $\bar{p}p$ Collisions at $\sqrt{s}$ =1.8 TeV*. PhD thesis, University of Chicago, December 2000.

[3] The CDF II Collaboration. The CDF II detector. Technical Design Report. FERMILAB-Pub- 96/390-E, Nov. 1996.

[4] D. Acosta et al. First measurements of inclusive w and z cross sections from run ii of the tevatron collider. *Phys. Rev. Lett.*, 94:091803, 2005.

[5] Victoria Martin. High-pt muon ID Cuts and Efficiencies for use with 5.3.1 Data and 5.3.3 MC. CDF Note 7367, Northwestern University, Nov. 19, 2004.

[6] Larry Nodulman. Curvature Corrections for 5.3.1 and 6.1.1. CDF Note 6971, Fermilab, 2005.

[7] Mircea Coca and Eva Halkiadakis. Central Electron Identification Efficiencies for the 200 pb^{-1} Run 2 Dataset. CDF Note 6580, University of Rochester, Jan. 6, 2004.

[8] Sam Harper and Greg Veramendy. Very High-Pt Electron Identification. CDF Note 7527, Fermilab, 2005.

[9] Mircea Coca and Eva Halkiadakis. Plug Electron Baseline Cuts Defined in Summer 2003 and Cut Efficiencies. CDF Note 6580, for the ETF group, Feb. 16, 2004.

[10] See: Baseline Analysis Cuts for High Pt Photons V2.3, http://www-cdf.fnal.gov/internal/physics/photon/docs/cuts.html.

[11] Torbjorn Sjostrand, Leif Lonnblad, and Stephen Mrenna. Pythia 6.2: Physics and manual. 2001.

[12] Heather K Gerberich, Ashutosh V. Kotwal and Chris Hays. Cosmic Ray Tagging using COT Hit Timing. CDF Note 6089, 2002.

[13] Peter B. Arnold and M. Hall Reno. The complete computation of high-p_t W and Z production in second-order QCD. *Nuclear Physics B*, (319):31–71, 1989.

[14] C. Balazs, J. Huston and I.Puljak. Higgs boson production: A comparison of parton showers and resummation. *Phys. Rev. D*, 63(014021), 2000.

[15] (The CDF Collaboration. First Measurement of Inclusive W and Z Cross Sections from Run II of the Tevatron Collider. *Phys. Rev. Lett.*, 94(091803), 2005. PRD numbers are not known yet.

[16] Joel Heinrich. User guide to bayesian-liimt software package. CDF Note 7232, 2004.

[17] See http://www-cdf.fnal.gov/physics/statistics/statistics_home.html.

[18] Joel Heinrich, Craig Blocker, John Conway, Luc Demortier, Louis Lyons, Giovani Punzi, Pekka K. Sinervo. Interval estimation on the presence of nuisance parameters. 1.Bayesian approach. *CDF Note*, (7117), 2004. http://xxx.lanl.gov/physics/0409129.

[19] J.D. Bjorken, S. Pakvasa, and S.F. Tuan. Yet Another Extension of the Standard Model: Oases in the Desert? *Phys. Rev. D*, 66(053008), 2002. http://xxx.lanl.gov/abs/hep-ph/0206116.

17 Appendices

Here we present a summary of observed events. The summary includes most of the Z + X events except some events from the Z+ H_T category. The category has too many entries so here we show only events with $H_T > 400$ GeV. In addition to that we list events with $P_T(Z) > 200$ GeV.

17.1 Summary of $Z \to ee$ events

17.1.1 $Z \to ee$, $P_T(Z) > 200$ GeV

Table 12: List of $Z \to ee$ events with $P_T(Z) > 200$ GeV.

	Leptons				Jets			Photons			$\not{E}_T$			Z	
run/event	p_T	η	ϕ	Type	p_T	η	ϕ	p_T	η	ϕ	p_T	ϕ	H_T	M(ll)	p_T
162130/3153429	183.07	-0.28	0.54	t, CEM	192.08	-0.05	4.13				14.22	3.76	490.54	91.73	240.28
	67.05	-0.81	1.18	t, CEM	52.33	-0.54	2.71								
					21.77	0.68	3.62								
185281/8932529	139.63	-0.39	4.02	t, CEM	149.93	-0.20	0.89				48.22	1.05	429.78	75.09	218.22
	78.65	-1.09	4.07	l, CEM	18.52	0.17	0.47								
207488/24091316	170.42	0.52	4.56	t, CEM	207.81	-0.66	1.77				8.27	1.52	476.46	88.35	228.38
	74.43	0.55	5.37	l, CEM	21.13	0.21	1.94								
210008/6429098	178.46	-0.08	1.37	t, CEM	320.63	-0.57	4.52				14.68	1.90	602.29	84.70	285.17
	106.82	0.52	1.43	t, CEM	21.28	-1.72	0.62								

17.1.2 $Z \to ee$, $H_T > 400$ GeV

Table 13: List of $Z \rightarrow ee$ events satisfying $H_T > 400$ GeV cut.

	Leptons				Jets			Photons			$\not\!\!E_T$			Z	
run/event	p_T	η	ϕ	Type	p_T	η	ϕ	p_T	η	ϕ	p_T	ϕ	H_T	M(ll)	p_T
162130/3153429	183.07	-0.28	0.54	t, CEM	192.08	-0.05	4.13				14.22	3.76	490.54	91.73	240.28
	67.05	-0.81	1.18	t, CEM	52.33	-0.54	2.71								
					21.77	0.68	3.62								
185281/8932529	139.63	-0.39	4.02	t, CEM	149.93	-0.20	0.89				48.22	1.05	429.78	75.09	218.22
	78.65	-1.09	4.07	l, CEM	18.52	0.17	0.47								
192282/5045814	192.23	-0.53	3.33	t, CEM	157.31	-0.63	0.12				23.12	0.30	406.22	90.58	197.57
	20.64	0.15	1.97	t, CEM	15.17	0.11	0.30								
204640/6474788	75.45	-0.51	3.12	t, CEM	65.21	-0.44	0.81				25.93	2.11	455.01	89.15	57.57
	21.55	0.51	0.49	t, CEM	17.05	1.06	4.22								
					16.04	1.26	3.77								
207488/24091316	170.42	0.52	4.56	t, CEM	207.81	-0.66	1.77				8.27	1.52	476.46	88.35	228.38
	74.43	0.55	5.37	l, CEM	21.13	0.21	1.94								
210008/6429098	178.46	-0.08	1.37	t, CEM	320.63	-0.57	4.52				14.68	1.90	602.29	84.70	285.17
	106.82	0.52	1.43	t, CEM	21.28	-1.72	0.62								

17.1.3 Z + Leptons

Table 14: List of "Z + Leptons" events. The leptons can be tight electrons or muons. The Z-bosons are reconstructed via $Z \rightarrow ee$ decay mode.

	Leptons				Jets			Photons			$\not\!\!E_T$			Z	
run/event	p_T	η	ϕ	Type	p_T	η	ϕ	p_T	η	ϕ	p_T	ϕ	H_T	M(ll)	p_T
184778/2248198	44.43	0.27	4.79	t, CEM							1.19	6.08	158.53	101.26	49.47
	44.00	-0.55	0.20	t, CEM											
	54.81	-0.76	2.68	l, CEM											

	Leptons				Jets			Photons			$\not\!\!E_T$			Z	
run/event	p_T	η	ϕ	Type	p_T	η	ϕ	p_T	η	ϕ	p_T	ϕ	H_T	M(ll)	p_T
185248/3266476	34.44	-0.29	0.29	t, CEM							8.77	1.08	131.27	93.16	24.72
	20.72	1.12	1.13	t, CEM											
	53.90	0.57	3.78	l, CEM											
196043/3035679	88.25	0.25	3.88	t, CEM	22.66	-0.09	1.34				46.44	0.05	203.07	81.99	82.05
	23.79	-0.39	1.91	t, CEM											
	22.21	0.33	0.63	t, CEM											

17.1.4 Z + $\not\!\!E_T$-signature

Table 15: List of events where Z is produced in assouciation with $\not\!\!E_T$-signature. The Z-bosons are reconstructed in $Z \to ee$ decay mode.

	Leptons				Jets			Photons			$\not\!\!E_T$			Z	
run/event	p_T	η	ϕ	Type	p_T	η	ϕ	p_T	η	ϕ	p_T	ϕ	H_T	M(ll)	p_T
178881/7124925	38.63	0.77	1.78	t, CEM	45.99	-1.13	6.01				37.49	4.42	182.39	101.25	70.80
	46.73	-1.06	2.97	l, CEM											
177214/4198401	39.26	0.69	0.17	t, CEM							28.92	2.72	95.99	78.73	27.16
	27.81	-0.70	4.08	t, CEM											
178677/611526	60.19	-0.54	3.71	t, CEM							57.46	1.35	158.39	85.20	54.28
	40.74	-0.63	5.78	t, CEM											
178677/3521141	79.64	-0.97	6.04	t, CEM	70.50	-0.90	3.01				34.21	2.62	215.25	100.30	110.94
	31.45	0.79	5.92	t, CEM											
178785/5665764	106.93	0.68	1.82	t, CEM	101.82	-1.33	5.44				33.08	5.18	268.41	88.05	124.36
	44.45	0.43	3.17	t, CEM	20.58	0.99	2.80								
150820/4167559	72.41	-0.74	2.80	t, CEM	32.85	-1.12	0.39				28.01	4.45	243.86	91.32	57.91
	15.35	0.95	6.24	l, CEM											
155796/250825	58.26	0.32	0.67	t, CEM	69.51	0.66	4.69				28.44	2.03	194.17	78.83	55.91
	38.18	0.19	2.64	t, CEM											

	Leptons				Jets			Photons			$\not\!\!E_T$			Z	
run/event	p_T	η	ϕ	Type	p_T	η	ϕ	p_T	η	ϕ	p_T	ϕ	H_T	M(ll)	p_T
156116/891235	68.97	0.76	3.24	t, CEM	56.48	0.42	0.85				27.92	0.41	202.67	91.55	75.92
	49.57	0.92	5.03	t, CEM											
160591/1383347	52.71	-0.73	2.31	t, CEM							26.25	5.12	100.75	68.82	30.93
	21.78	-1.08	5.47	l, CEM											
153416/2941045	44.47	0.59	3.76	t, CEM							25.18	0.75	84.19	66.20	29.97
	14.55	-0.93	0.55	l, CEM											
155712/57220	25.05	-0.54	3.11	t, CEM							32.86	3.33	141.50	84.93	47.14
	71.28	-0.25	0.19	l, CEM											
161678/5620107	67.28	-0.52	4.78	t, CEM							36.10	2.28	151.46	109.15	37.34
	48.08	-0.51	1.07	t, CEM											
164844/336757	58.51	-0.91	1.03	t, CEM							37.25	4.24	116.41	69.92	37.93
	20.64	-1.13	4.23	l, CEM											
167996/1173352	38.01	-1.03	1.74	t, CEM							68.11	4.68	136.30	78.51	62.86
	30.18	0.86	0.94	t, CEM											
167053/12891960	50.54	-0.75	3.73	t, CEM							53.31	1.31	139.96	93.40	34.96
	36.11	0.35	6.10	t, CEM											
184310/4602801	57.20	-0.66	1.33	t, CEM							37.10	3.64	150.78	105.88	48.74
	56.48	-0.21	5.36	t, CEM											
184466/383360	89.94	0.43	4.78	t, CEM	53.88	0.13	0.87				93.11	0.92	248.01	109.43	70.16
	37.80	0.84	2.47	l, CEM	50.12	1.43	3.48								
					18.97	-1.29	4.97								
					16.73	-1.09	4.52								
184377/1063301	48.28	0.38	3.54	t, CEM	39.57	0.62	1.71				25.55	0.03	147.81	74.70	37.85
	35.14	0.56	5.79	t, CEM											
184778/2016279	55.83	-0.58	2.24	t, CEM	37.62	-0.36	4.17				27.11	5.84	143.76	66.59	45.60
	23.62	-0.97	0.02	t, CEM											
184802/5465538	55.20	0.81	1.81	t, CEM							28.93	5.04	109.28	74.66	30.05
	25.15	0.93	4.95	t, CEM											

	Leptons				Jets			Photons			$\not\!\!E_T$			Z	
run/event	p_T	η	ϕ	Type	p_T	η	ϕ	p_T	η	ϕ	p_T	ϕ	H_T	M(ll)	p_T
185172/6375050	51.10	-0.18	5.53	t, CEM	16.04	1.67	5.70				44.50	2.53	137.02	71.40	32.93
	25.45	0.31	1.80	l, CEM											
168600/151628	59.56	-0.26	2.56	t, CEM							40.69	6.01	130.12	83.13	38.1[illegible]
	29.88	-0.71	5.13	l, CEM											
186302/1350884	44.19	0.57	2.65	t, CEM							29.49	5.49	89.25	68.58	31.82
	15.57	-1.02	5.25	l, CEM											
185280/1260045	82.13	0.01	5.41	t, CEM	165.03	-0.81	1.74				42.61	4.65	348.93	86.25	127.36
	60.25	-0.80	4.47	t, CEM											
185281/8932529	139.63	-0.39	4.02	t, CEM	149.93	-0.20	0.89				48.22	1.05	429.78	75.09	218.22
	78.65	-1.09	4.07	l, CEM	18.52	0.17	0.47								
185331/2000738	50.89	-0.65	2.84	t, CEM							31.24	6.10	105.43	77.20	27.66
	23.29	0.33	5.93	l, CEM											
185594/9511456	74.22	0.86	1.73	t, CEM							49.84	4.89	148.59	85.32	49.85
	24.53	0.78	4.78	t, CEM											
185542/3003816	21.86	-0.80	3.20	t, CEM	43.03	0.10	4.14				49.11	4.26	184.20	85.31	75.98
	92.37	-0.76	0.70	l, CEM	25.48	-1.12	1.37								
196275/6002858	121.53	0.17	2.50	t, CEM	58.34	0.31	5.42				63.75	5.51	269.88	95.47	124.49
	26.81	-0.70	0.93	t, CEM											
196276/3385454	58.13	-0.28	1.80	t, CEM	21.24	0.83	1.88				39.35	5.46	158.32	113.56	25.39
	39.98	0.94	4.57	l, CEM											
196354/3069410	72.94	-0.21	2.41	t, CEM	80.28	-1.27	5.49	36.34	-0.82	5.00	37.92	2.14	225.61	86.76	52.18
	25.24	0.36	6.05	t, CEM	50.06	-0.86	4.98								
					23.92	0.30	2.56								
					15.53	-0.66	2.09								
195742/5097617	41.60	0.30	2.11	t, CEM							28.97	5.43	112.27	69.68	15.17
	28.50	0.68	5.48	t, CEM											
196043/3035679	88.25	0.25	3.88	t, CEM	22.66	-0.09	1.34				46.44	0.05	203.07	81.99	82.05
	23.79	-0.39	1.91	t, CEM											
	22.21	0.33	0.63	t, CEM											

	Leptons				Jets			Photons			$\not{E}_T$			Z	
run/event	p_T	η	ϕ	Type	p_T	η	ϕ	p_T	η	ϕ	p_T	ϕ	H_T	M(ll)	p_T
196099/7758852	77.50	-0.87	4.78	t, CEM	32.20	0.48	2.05				31.06	2.20	164.34	91.70	54.93
	29.27	-0.76	1.08	l, CEM	15.28	-0.02	5.18								
197763/2869755	52.12	-0.25	5.36	t, CEM	67.23	0.03	4.36				29.60	1.56	157.83	91.62	34.45
	34.82	0.76	1.51	l, CEM	42.62	-0.79	1.85								
197194/7220786	55.10	-0.31	3.50	t, CEM	59.77	-0.44	5.51				26.37	1.10	168.30	69.27	46.26
	27.44	-0.59	1.36	l, CEM											
197287/1724640	47.20	0.18	0.62	t, CEM							35.43	1.53	149.77	110.21	33.98
	67.14	0.45	4.26	l, CEM											
199025/12207958	79.82	-0.92	1.29	t, CEM	20.67	1.39	3.45				27.50	4.68	161.35	103.08	46.97
	33.44	-0.96	4.58	t, CEM											
199559/6818215	69.91	-0.54	3.54	t, CEM	18.97	0.25	5.73				27.98	0.74	236.35	101.60	45.34
	24.66	0.78	0.33	l, CEM	16.21	1.41	4.58								
198613/1063988	45.57	-0.55	1.14	t, CEM							26.48	4.48	110.88	86.98	6.82
	38.83	-0.03	4.30	t, CEM											
198623/1383967	42.54	-0.59	3.72	t, CEM	63.82	-0.89	5.60				30.43	2.53	222.42	87.86	65.01
	59.10	0.19	1.93	l, CEM	35.43	-0.80	6.22								
200570/2423417	61.52	0.64	3.34	t, CEM							28.83	0.28	118.26	90.65	34.05
	27.91	-0.23	0.07	t, CEM											
200756/511767	52.89	-0.77	4.31	t, CEM	42.89	0.67	1.29				26.72	1.97	157.20	92.78	64.87
	35.36	0.73	5.84	t, CEM											
201154/1363671	22.74	0.75	1.59	t, CEM							25.04	1.49	97.23	67.27	26.92
	49.45	0.57	4.63	l, CEM											
191208/44206	51.41	-0.83	5.03	t, CEM	115.62	0.88	1.58				55.22	1.59	303.22	92.89	148.92
	101.48	0.30	4.55	l, CEM	20.94	1.48	5.00								
193032/1657759	69.82	0.41	4.58	t, CEM	37.29	1.46	0.89				73.22	2.15	207.24	90.12	91.65
	43.81	-0.63	5.88	t, CEM	17.12	-0.09	3.95								
191803/265771	93.63	-0.96	2.18	t, CEM	52.83	-0.82	5.01				29.97	4.97	206.46	99.97	78.62
	30.87	-0.48	6.24	t, CEM											

	Leptons				Jets			Photons			$\not\!\!E_T$			Z	
run/event	p_T	η	ϕ	Type	p_T	η	ϕ	p_T	η	ϕ	p_T	ϕ	H_T	M(ll)	p_T
192345/8656726	52.84	0.50	2.03	t, CEM							28.44	5.05	105.76	72.05	35.68
	24.47	1.10	5.78	t, CEM											
192348/546099	34.89	-0.07	1.34	t, CEM	22.96	-1.37	1.12				41.26	4.21	154.62	71.25	1.68
	35.46	-0.39	4.43	l, CEM	20.81	-2.35	0.77								
192348/7020043	86.44	-0.24	1.40	t, CEM	47.67	0.18	4.98				50.27	5.07	201.00	95.10	80.77
	29.63	0.64	3.33	t, CEM	35.93	-1.21	4.60								
					30.98	0.44	1.77								
					16.99	-0.68	1.86								
194813/1822069	51.52	0.83	1.36	t, CEM	25.71	-2.09	0.88				26.42	5.13	140.02	100.84	4.98
	46.81	0.37	4.47	t, CEM	23.59	-0.94	4.02								
194862/13214870	87.77	-0.49	5.14	t, CEM							68.04	2.28	181.72	89.75	70.56
	25.90	-0.28	1.28	t, CEM											
202003/454339	42.24	0.18	3.02	t, CEM							32.78	5.28	120.58	70.24	22.98
	25.76	-0.67	0.37	t, CEM											
202041/3723850	38.46	-0.11	4.17	t, CEM	27.63	-2.14	1.29				26.42	4.61	118.33	67.35	12.58
	25.88	-0.84	1.03	t, CEM											
202070/407060	93.06	0.39	1.39	t, CEM	40.89	-1.37	5.47				34.80	3.58	267.03	95.84	91.17
	38.60	0.17	5.84	t, CEM											
	59.77	-1.11	3.55	l, CEM											
202070/514646	56.98	0.68	4.04	t, CEM	62.17	0.10	2.21				73.50	5.79	218.19	82.29	32.51
	26.87	-0.02	1.21	t, CEM											
202135/160111	58.01	-0.98	5.69	t, CEM	73.55	0.86	5.30				30.99	2.27	122.45	86.55	35.07
	22.97	0.22	2.58	t, CEM	41.32	0.55	1.95								
					32.87	1.70	2.62								
202513/212024	99.28	0.14	3.52	t, CEM							103.52	0.71	229.07	82.08	103.83
	26.27	-0.66	5.05	t, CEM											
202697/4844482	181.22	-0.67	5.05	t, CEM	124.76	-0.27	1.77				45.38	1.71	382.82	88.75	184.42
	22.93	-0.45	3.56	t, CEM	19.51	-1.74	2.68								

	Leptons				Jets			Photons			$\not{E}_T$			Z	
run/event	p_T	η	ϕ	Type	p_T	η	ϕ	p_T	η	ϕ	p_T	ϕ	H_T	M(ll)	p_T
203190/3666112	30.92	0.86	0.19	t, CEM	120.24	0.15	4.27				26.05	4.02	129.72	87.00	30.47
	49.02	-0.26	2.69	l, CEM	101.88	2.18	0.94								
					20.64	-1.29	2.25								
					18.24	-0.81	5.61								
203265/13675248	38.11	-0.59	2.60	t, CEM	48.66	1.00	4.76				31.72	1.32	129.33	90.43	14.84
	36.55	0.73	5.34	t, CEM	27.06	0.49	1.41								
203265/3792931	123.91	-0.34	0.99	t, CEM							177.80	3.90	353.32	92.42	161.40
	51.61	-1.10	0.10	t, CEM											
203764/1850579	45.02	-0.56	3.88	t, CEM	16.91	-1.22	2.98				103.03	1.39	251.75	87.84	76.69
	69.31	-0.97	5.60	l, CEM											
204679/1692937	65.71	0.63	3.95	t, CEM	32.77	0.26	2.80				26.63	0.50	154.04	87.64	44.43
	32.18	0.81	0.16	t, CEM	16.10	-0.62	0.17								
203881/12606468	75.49	-0.68	4.17	t, CEM	74.50	-0.20	1.85				36.61	1.48	258.88	94.88	114.63
	72.70	-0.50	5.54	l, CEM											
204444/1961053	39.24	0.00	1.54	t, CEM	24.71	-1.68	0.06				27.37	3.17	142.24	91.62	14.52
	43.77	0.96	5.02	l, CEM											
204921/98566	34.44	-0.32	4.24	t, CEM							26.16	1.47	110.07	70.78	7.60
	29.96	0.59	1.29	t, CEM											
206029/83826	57.19	0.13	3.75	t, CEM	22.86	1.72	2.94				36.31	0.62	148.89	90.07	25.11
	35.03	0.47	0.35	t, CEM	16.38	-0.19	0.59								
206033/2759014	45.94	-0.40	1.44	t, CEM	29.03	-1.06	4.15				32.95	3.96	151.22	87.99	70.02
	43.37	1.01	0.10	t, CEM											
206174/587851	47.08	0.54	3.64	t, CEM							58.71	5.09	153.20	103.15	38.94
	46.32	-0.65	1.35	t, CEM											
206174/4754829	45.90	0.20	2.77	t, CEM	35.16	1.62	0.83				25.63	0.91	141.36	92.25	20.39
	34.81	-0.96	5.48	t, CEM											
206283/921459	47.11	0.27	3.58	t, CEM							31.34	0.60	101.84	66.77	23.84
	23.38	0.50	0.50	t, CEM											

	Leptons				Jets			Photons			$\not\!\!E_T$			Z	
run/event	p_T	η	ϕ	Type	p_T	η	ϕ	p_T	η	ϕ	p_T	ϕ	H_T	M(ll)	p_T
206537/6028547	94.28	-1.00	5.22	t, CEM	60.67	-0.10	1.86				26.74	2.14	209.58	98.78	74.6[illegible]
	29.35	-0.88	2.79	l, CEM											
206982/882173	48.59	0.54	4.03	t, CEM							25.08	0.17	131.96	89.08	11.9[illegible]
	41.06	0.40	1.09	t, CEM											
206989/7534690	21.45	0.75	4.47	t, CEM	60.04	0.19	5.28				28.77	1.81	222.73	69.36	68.08
	75.74	0.74	2.40	l, CEM	34.26	-0.33	5.31								
205624/3517000	44.92	-0.56	5.96	t, CEM	48.61	-1.02	0.57				30.53	3.30	166.28	87.38	6.21
	42.54	-0.67	2.69	t, CEM											
209263/5476924	42.94	-0.05	0.14	t, CEM	15.04	0.95	6.07				28.93	2.54	127.46	89.00	25.00
	40.70	0.86	3.89	t, CEM											
209021/4038281	145.43	0.35	2.07	t, CEM							139.22	5.09	310.89	92.70	145.28
	26.24	0.10	0.40	t, CEM											
207488/22697904	120.18	-0.79	4.04	t, CEM	67.39	0.07	1.12				25.91	1.14	240.66	92.02	118.28
	27.73	-0.37	5.80	t, CEM											
209265/2059240	48.34	0.70	2.30	t, CEM							27.21	5.21	101.09	70.33	22.97
	25.54	0.59	5.51	t, CEM											
209402/2463065	58.33	0.03	2.72	t, CEM	23.22	-1.89	4.62				25.97	5.69	159.86	100.46	50.58
	41.35	1.05	0.59	t, CEM	18.49	-0.67	3.41								
209437/1763481	58.93	0.01	1.25	t, CEM	100.81	-0.31	3.50				27.76	5.65	240.24	87.63	87.48
	53.39	0.91	6.17	t, CEM											
209439/2854881	46.90	0.03	4.36	t, CEM							68.97	0.32	176.08	81.03	72.46
	60.21	0.38	2.69	l, CEM											
209439/3255646	34.80	-0.61	1.81	t, CEM	41.15	0.30	1.52				94.74	4.62	215.73	68.01	42.77
	27.19	0.90	0.17	l, CEM	35.44	0.05	0.63								
					21.74	0.85	3.11								
209486/1242753	41.40	0.37	1.36	t, CEM							26.38	5.59	130.40	91.44	10.67
	41.28	-0.57	4.24	l, CEM											
209986/23045716	42.39	0.61	1.41	t, CEM							29.55	4.60	111.10	68.34	15.31
	27.58	0.53	4.43	t, CEM											

	Leptons				Jets			Photons			$\not\!\!E_T$			Z	
run/event	p_T	η	ϕ	Type	p_T	η	ϕ	p_T	η	ϕ	p_T	ϕ	H_T	M(ll)	p_T
210008/7652752	50.66	-0.06	0.50	t, CEM	59.70	-1.10	0.17				70.53	3.19	235.75	84.47	49.67
	46.47	0.20	2.57	t, CEM	32.47	0.91	5.12								
					23.40	0.69	4.03								
210008/9625876	52.94	-0.16	4.74	t, CEM							27.75	2.00	113.04	84.69	20.69
	32.35	0.27	1.65	t, CEM											
209762/3023411	46.56	-0.33	1.73	t, CEM							25.19	5.46	122.68	91.66	11.60
	38.96	0.47	4.67	l, CEM											
209819/6110743	62.34	-0.92	3.26	t, CEM	19.01	-0.52	0.99				29.48	0.66	142.20	84.33	48.84
	31.62	-0.35	5.52	t, CEM											
209850/1589151	24.01	-0.28	2.52	t, CEM	19.83	0.78	2.51				26.72	2.46	136.14	93.06	42.31
	65.91	0.88	5.52	l, CEM											
211337/2890896	47.66	0.91	2.85	t, CEM							27.56	0.82	155.48	92.03	16.33
	44.74	0.61	0.06	t, CEM											
211441/4654904	45.26	-0.64	3.09	t, CEM							25.17	0.88	129.65	90.21	2.66
	44.68	-0.81	6.17	t, CEM											
211903/10178296	80.16	0.62	1.91	t, CEM	44.95	0.70	4.68				26.54	4.50	162.11	86.91	60.64
	23.88	0.16	5.57	t, CEM	26.97	-0.40	0.78								
210914/4179741	30.19	0.62	0.86	t, CEM	84.22	-1.26	2.29				29.58	5.16	186.19	77.66	40.22
	57.17	0.72	4.73	l, CEM	23.17	-0.67	6.19								
211198/10464833	64.31	0.06	0.05	t, CEM	40.17	-1.84	2.83				35.92	3.08	153.93	72.11	58.25
	25.73	0.60	2.06	t, CEM	40.97	0.20	5.77								
					20.30	1.72	4.70								
211198/12842685	44.46	-0.94	3.87	t, CEM	29.83	0.74	5.76				40.50	1.72	145.39	82.42	14.13
	30.82	0.01	0.82	t, CEM											

17.1.5 Z + Photons

Table 16: List of "Z + Photon" events. The Z-boson is reconstructed in $Z \to ee$ decay mode.

	Leptons				Jets			Photons			$\not\!\!E_T$			Z	
run/event	p_T	η	ϕ	Type	p_T	η	ϕ	p_T	η	ϕ	p_T	ϕ	H_T	M(ll)	p_T
178602/3018939	60.24	-0.77	5.60	t, CEM				25.72	-0.92	2.74	5.99	4.76	124.71	110.57	29.33
	32.77	0.62	2.23	t, CEM											
178852/3194148	101.66	0.45	0.58	t, CEM	117.90	0.48	3.38	94.25	0.44	3.36	23.13	0.07	274.12	85.97	101.71
	31.52	0.45	5.14	l, CEM											
152745/380176	21.82	0.58	5.78	t, CEM				57.42	0.76	4.61	18.08	3.05	156.85	92.35	53.93
	59.52	-1.13	1.51	l, CEM											
164844/6642760	57.45	0.89	3.37	t, CEM				26.85	-0.07	5.62	9.70	1.93	135.01	95.96	22.5[illegible]
	41.01	0.99	0.54	t, CEM											
196354/3069410	72.94	-0.21	2.41	t, CEM	80.28	-1.27	5.49	36.34	-0.82	5.00	37.92	2.14	225.61	86.76	52.18
	25.24	0.36	6.05	t, CEM	50.06	-0.86	4.98								
					23.92	0.30	2.56								
					15.53	-0.66	2.09								
198082/3483348	44.38	0.72	4.95	t, CEM				27.63	-1.07	1.11	2.88	0.62	103.61	88.21	31.36
	28.72	-0.78	2.59	t, CEM											
197079/7457253	58.24	0.03	3.87	t, CEM				97.23	0.73	1.45	6.96	6.26	222.62	93.84	96.00
	60.19	1.05	5.12	l, CEM											
199025/10197457	56.65	0.43	2.55	t, CEM				45.52	0.94	5.05	6.64	1.77	144.41	89.99	36.62
	35.59	-0.23	0.09	t, CEM											
199559/11744671	127.85	0.86	4.88	t, CEM	19.77	0.74	3.43	111.14	0.18	1.69	7.79	6.19	286.04	89.05	137.11
	19.51	-0.46	3.74	l, CEM											
200661/380979	66.62	0.39	1.46	t, CEM	19.73	1.94	1.19	57.95	-0.30	4.59	4.63	5.43	173.71	84.38	41.91
	24.80	0.94	4.67	t, CEM											
191640/2188456	88.90	-0.41	3.70	t, CEM				66.77	-1.01	0.23	2.61	5.21	188.49	91.57	78.22
	30.20	-0.07	1.60	t, CEM											
199725/3343816	45.42	-0.09	4.12	t, CEM				28.01	-0.50	5.98	3.11	2.44	132.62	90.30	18.27
	45.57	-0.41	1.38	l, CEM											

	Leptons				Jets			Photons			$\not\!\!E_T$			Z	
run/event	p_T	η	ϕ	Type	p_T	η	ϕ	p_T	η	ϕ	p_T	ϕ	H_T	M(ll)	p_T
209052/1717093	64.03	0.26	2.25	t, CEM	87.97	-1.63	5.28	95.54	0.63	1.00	15.10	3.85	320.20	90.36	82.57
	58.10	0.39	3.91	t, CEM											
209372/1209547	77.29	-0.37	3.04	t, CEM				73.25	0.41	5.71	4.95	3.15	191.92	91.60	68.51
	36.43	-0.13	0.99	t, CEM											

17.2 Summary of $Z \to \mu\mu$ events

17.2.1 $Z \to \mu\mu$, $P_T(Z) > 200$ GeV

Table 17: List of $Z \to \mu\mu$ events with $P_T(Z) > 200$ GeV.

	Leptons				Jets			Photons			$\not\!\!E_T$			Z	
run/event	p_T	η	ϕ	Type	p_T	η	ϕ	p_T	η	ϕ	p_T	ϕ	H_T	M(ll)	p_T
163064/1946231	144.21	-0.07	-1.87	t, CMUP	170.93	-0.05	1.05				60.20	0.91	474.87	89.81	236.62
	108.87	-0.09	-2.60	l	15.61	-0.31	5.82								
183617/1437485	128.46	-0.36	-2.32	t, CMUP	186.77	-0.31	0.53				31.64	0.72	431.39	100.26	216.73
	94.48	-1.12	-2.80	l											
184414/3419885	194.94	0.30	-0.55	t, CMUP	73.51	0.72	2.48				14.05	5.39	459.33	92.65	215.57
	24.95	-0.82	0.08	t, CMX	66.39	1.19	2.67								
					50.07	0.12	2.54								
					41.33	-2.08	3.01								
185594/1789040	72.98	0.36	-1.46	t, CMUP	225.97	0.27	2.05				36.42	2.66	545.15	97.26	265.83
	207.72	0.66	-0.71	l	20.57	0.53	3.97								
196354/3749647	169.42	0.81	0.96	t, CMX	252.34	-0.37	3.91				23.02	3.71	516.62	90.52	251.87
	93.90	0.43	0.34	t, CMUP											
197189/528661	164.20	0.46	1.16	t, CMUP	243.43	-0.88	4.44				10.54	0.86	499.72	84.37	240.03
	82.14	-0.08	1.64	t, CMUP											
198082/3090011	160.40	0.26	2.05	t, CMUP	267.52	0.08	5.47				10.02	5.17	571.15	80.79	283.39
	134.03	0.18	2.60	t, CMUP											
194266/1431107	218.96	-0.17	1.42	t, CMUP	176.62	-0.08	5.00				55.74	4.84	559.42	101.17	273.80
	70.31	-0.48	2.19	t, CMUP	39.64	0.86	4.55								
					27.61	-0.79	3.11								
202136/2606913	71.20	0.02	-2.77	t, CMUP	221.31	-0.32	0.90				3.54	1.58	443.16	86.71	218.82
	164.08	0.08	-1.95	l											
202526/822310	141.40	0.18	1.09	t, CMUP	184.43	-0.98	4.08				16.07	4.51	412.32	89.81	209.26
	71.16	0.97	0.72	l											

	Leptons				Jets			Photons			$\not\!\!E_T$			Z	
run/event	p_T	η	ϕ	Type	p_T	η	ϕ	p_T	η	ϕ	p_T	ϕ	H_T	M(ll)	p_T
204750/1803713	85.79	0.31	1.44	t, CMUP	190.57	0.75	4.02				64.26	4.17	533.15	93.26	263.69
	193.90	0.30	0.70	l											

17.2.2 $Z \to \mu\mu$, $H_T > 400$ GeV

Table 18: List of $Z \to \mu\mu$ events with $H_T > 400$ GeV.

	Leptons				Jets			Photons			$\not\!\!E_T$			Z	
run/event	p_T	η	ϕ	Type	p_T	η	ϕ	p_T	η	ϕ	p_T	ϕ	H_T	M(ll)	p_T
163064/1946231	144.21	-0.07	-1.87	t, CMUP	170.93	-0.05	1.05				60.20	0.91	474.87	89.81	236.62
	108.87	-0.09	-2.60	l	15.61	-0.31	5.82								
183617/1437485	128.46	-0.36	-2.32	t, CMUP	186.77	-0.31	0.53				31.64	0.72	431.39	100.26	216.73
	94.48	-1.12	-2.80	l											
184414/3419885	194.94	0.30	-0.55	t, CMUP	73.51	0.72	2.48				14.05	5.39	459.33	92.65	215.57
	24.95	-0.82	0.08	t, CMX	66.39	1.19	2.67								
					50.07	0.12	2.54								
					41.33	-2.08	3.01								
185594/1789040	72.98	0.36	-1.46	t, CMUP	225.97	0.27	2.05				36.42	2.66	545.15	97.26	265.83
	207.72	0.66	-0.71	l	20.57	0.53	3.97								
196354/3749647	169.42	0.81	0.96	t, CMX	252.34	-0.37	3.91				23.02	3.71	516.62	90.52	251.87
	93.90	0.43	0.34	t, CMUP											
197189/528661	164.20	0.46	1.16	t, CMUP	243.43	-0.88	4.44				10.54	0.86	499.72	84.37	240.03
	82.14	-0.08	1.64	t, CMUP											
198082/3090011	160.40	0.26	2.05	t, CMUP	267.52	0.08	5.47				10.02	5.17	571.15	80.79	283.39
	134.03	0.18	2.60	t, CMUP											
194266/1431107	218.96	-0.17	1.42	t, CMUP	176.62	-0.08	5.00				55.74	4.84	559.42	101.17	273.80
	70.31	-0.48	2.19	t, CMUP	39.64	0.86	4.55								
					27.61	-0.79	3.11								

	Leptons				Jets			Photons			$\not\!\!E_T$			Z	
run/event	p_T	η	ϕ	Type	p_T	η	ϕ	p_T	η	ϕ	p_T	ϕ	H_T	M(ll)	p_T
202136/2606913	71.20	0.02	-2.77	t, CMUP	221.31	-0.32	0.90				3.54	1.58	443.16	86.71	218.82
	164.08	0.08	-1.95	l											
202526/822310	141.40	0.18	1.09	t, CMUP	184.43	-0.98	4.08				16.07	4.51	412.32	89.81	209.26
	71.16	0.97	0.72	l											
204750/1803713	85.79	0.31	1.44	t, CMUP	190.57	0.75	4.02				64.26	4.17	533.15	93.26	263.69
	193.90	0.30	0.70	l											

17.2.3 Z + Leptons

Table 19: List of "Z + Leptons" events. The leptons can be tight electrons or muons. The Z-bosons are reconstructed with $Z \to \mu\mu$ decay mode.

	Leptons				Jets			Photons			$\not\!\!E_T$			Z	
run/event	p_T	η	ϕ	Type	p_T	η	ϕ	p_T	η	ϕ	p_T	ϕ	H_T	M(ll)	p_T
185332/5307745	27.43	1.07	4.99	t, CEM							10.45	5.90	115.82	90.08	24.53
	45.02	0.00	1.48	t, CMUP											
	32.92	1.25	-2.22	l											
203015/1791462	31.91	1.05	5.31	t, CEM							4.79	6.01	139.07	96.26	38.51
	64.98	0.15	2.74	t, CMUP											
	37.39	-0.18	0.15	t, CMUP											

17.2.4 Z + $\not\!\!E_T$-signature

Table 20: List of events where Z-boson is produced in assouciation with $\not\!\!E_{\mathrm{T}}$-signature. The Z-bosons are reconstructed in $Z \rightarrow \mu\mu$ decay mode.

	Leptons				Jets			Photons			$\not\!\!E_{\mathrm{T}}$			Z	
run/event	p_{T}	η	ϕ	Type	p_{T}	η	ϕ	p_{T}	η	ϕ	p_{T}	ϕ	H_T	M(ll)	p_{T}
177480/740689	36.53	-0.42	-0.49	t, CMUP	51.67	0.18	1.32				37.13	1.38	238.56	93.57	103.67
	100.63	0.01	-2.16	l											
177938/1526966	44.54	0.40	-0.94	t, CMUP							25.80	2.27	94.73	68.34	20.26
	24.39	-0.14	2.26	t, CMUP											
178258/924382	43.48	0.93	3.14	t, CMX	24.25	1.24	5.20				27.11	5.16	118.92	94.60	33.31
	31.37	-0.69	0.86	t, CMX											
178540/2208375	64.41	-0.17	0.75	t, CMUP	97.86	0.24	3.86				53.03	0.32	252.40	94.95	49.88
	34.75	0.67	-1.52	l	44.07	0.70	2.15								
178758/4457978	62.08	-0.24	-0.41	t, CMUP	31.23	-0.20	4.20				26.25	3.99	160.47	92.43	60.72
	47.66	-0.49	1.58	l	25.62	-1.26	1.86								
155920/171026	33.51	-0.92	-0.68	t, CMX	49.43	1.78	3.61				25.56	0.25	135.93	88.58	8.10
	41.14	0.31	2.54	l	15.22	0.89	0.10								
155996/117916	54.33	-0.44	-2.54	t, CMUP							27.44	0.60	150.09	93.92	16.51
	40.87	-0.55	0.80	l											
160151/842563	60.31	0.28	2.91	t, CMUP							58.55	5.48	154.29	72.20	63.49
	35.43	0.48	1.14	t, CMUP											
154654/7344016	59.35	0.76	-3.13	t, CMX	37.57	0.29	4.82				56.36	0.40	239.91	70.66	87.68
	52.90	0.60	1.80	t, CMUP	20.65	-0.70	5.27								
					15.84	-0.22	4.83								
160823/1925	35.50	0.45	0.20	t, CMUP							40.90	2.35	129.82	91.21	47.53
	39.43	-1.23	-1.57	l											
161722/330583	39.02	-0.77	2.41	t, CMX							26.32	4.78	97.75	84.00	24.26
	32.41	0.55	-0.06	l											
162631/120026	84.76	-0.51	2.74	t, CMUP	18.09	-0.56	1.83				118.07	6.12	265.03	83.85	101.24
	44.46	-0.12	-2.12	l											

	Leptons				Jets			Photons			$\not\!\!E_T$			Z	
run/event	p_T	η	ϕ	Type	p_T	η	ϕ	p_T	η	ϕ	p_T	ϕ	H_T	M(ll)	p_T
163064/11651832	71.40 32.06	-0.73 -0.97	1.90 -1.94	t, CMX l	17.13	0.32	5.32				25.71	5.62	145.87	90.65	51.19
165297/4078686	60.87 33.14	-0.38 -1.00	-0.71 2.86	t, CMUP l	73.94 30.74 28.96	-2.02 -1.85 0.07	3.04 2.05 5.99				35.98	6.11	203.16	92.22	33.61
165388/2351554	43.41 41.25	-0.30 0.54	0.66 -2.39	t, CMUP l							27.86	6.09	139.25	92.26	4.27
165873/6965206	54.05 31.73	-0.72 0.22	2.96 0.19	t, CMX t, CMUP	38.14 28.83 23.88	1.71 -0.77 1.85	6.25 0.21 4.04				25.56	3.52	164.36	90.78	27.21
163431/3303080	34.74 39.71	-0.72 1.01	1.20 -0.69	t, CMX l	90.41	0.57	3.29				26.43	0.13	191.26	94.45	43.82
166715/1690893	40.29 39.74	0.30 0.82	1.82 -2.50	t, CMUP t, CMX							45.85	6.26	125.88	69.88	44.31
183617/986800	21.63 82.47	0.45 -0.85	1.13 -1.99	t, CMUP l	18.11	-1.75	0.94				41.52	1.43	163.68	103.05	60.85
184234/1621128	80.86 30.52	0.80 -0.23	-0.68 2.36	t, CMX l	39.91	-1.25	1.58				41.56	3.55	192.68	112.91	50.63
185542/4426671	60.34 38.05	-0.34 -1.20	2.27 0.55	t, CMUP l	96.96 17.65 17.99	-0.40 -0.83 -0.92	5.47 5.31 2.96				47.18	3.03	245.42	84.01	66.52
186084/431935	58.00 33.48	0.12 -0.31	-2.98 0.04	t, CMUP t, CMUP							25.33	0.19	116.81	90.02	25.11
186145/2035671	49.74 44.30	-0.02 0.56	-2.74 2.05	t, CMUP l	71.06	-0.16	0.27				39.37	4.74	204.21	69.71	68.86
185777/2836008	56.17 33.54	0.08 0.45	-0.93 2.58	t, CMUP l							30.71	1.69	120.43	86.88	27.74
185542/12204721	61.07 39.28	-0.36 -0.70	-0.94 0.54	t, CMUP t, CMX	78.77 76.00	-0.11 1.09	5.72 2.60				49.79	2.46	164.03	68.24	75.45

	Leptons				Jets			Photons			$\not\!\!E_{\mathrm{T}}$			Z	
run/event	p_{T}	η	ϕ	Type	p_{T}	η	ϕ	p_{T}	η	ϕ	p_{T}	ϕ	H_T	M(ll)	p_{T}
185542/2703807	51.75	-0.27	-2.98	t, CMUP							25.72	6.16	126.37	89.76	17.12
	39.14	-0.06	0.42	t, CMUP											
185377/103906	20.88	0.44	-1.73	t, CMUP	71.39	-0.32	5.84				79.52	3.02	271.67	79.66	55.54
	76.03	0.28	1.57	l	28.30	-2.33	5.30								
196043/3994453	131.69	-0.19	1.47	t, CMUP	92.63	-1.61	4.51				62.80	5.03	302.09	104.45	139.70
	41.26	-0.50	2.99	t, CMUP	33.14	0.17	0.85								
196085/5882848	39.66	-0.30	1.50	t, CMUP							28.02	3.30	124.39	88.72	58.40
	56.72	0.61	-0.39	l											
196170/553958	34.47	0.94	-0.11	t, CMX	77.60	0.33	0.05				54.30	2.38	158.68	84.65	42.67
	41.56	-0.44	-2.08	l	58.12	0.20	2.88								
196663/714179	61.08	-0.23	2.40	t, CMUP	30.23	0.30	5.98				56.81	4.49	176.11	99.36	42.07
	36.59	-1.16	-0.01	l	25.75	-0.80	1.19								
					20.59	-2.33	3.79								
196663/1068873	59.12	-0.69	-2.59	t, CMX	78.09	-0.00	0.08				28.33	3.50	190.91	88.56	27.01
	32.86	-0.93	0.41	t, CMX											
196737/3398117	28.47	0.24	-0.42	t, CMUP							35.62	5.81	117.61	78.81	25.06
	53.53	0.52	2.71	l											
197808/6530989	33.78	0.51	-1.63	t, CMUP	40.25	1.08	6.05				63.09	1.42	211.79	67.65	68.00
	57.85	1.14	3.12	l	20.88	1.61	5.30								
198882/1757363	27.12	-0.29	-1.12	t, CMUP	29.88	-1.64	3.10				45.23	5.26	169.02	76.67	34.48
	56.57	-0.49	1.56	l											
199187/2233097	35.30	0.40	-0.35	t, CMUP	120.56	0.02	4.14				44.32	1.02	275.28	87.66	73.08
	75.49	0.92	1.53	l											
200027/48164	64.00	-0.09	1.15	t, CMUP	94.08	-0.79	3.82				38.57	1.04	241.08	81.83	69.33
	37.74	0.58	-0.57	l											

	Leptons				Jets			Photons			$\not\!\!E_T$			Z	
run/event	p_T	η	ϕ	Type	p_T	η	ϕ	p_T	η	ϕ	p_T	ϕ	H_T	M(ll)	p_T
191545/898092	58.75	0.31	1.60	t, CMUP	79.66	0.55	2.56				45.49	4.08	159.80	87.51	29.97
	33.64	0.21	-1.18	t, CMUP	64.96	-0.96	6.27								
					20.39	0.31	6.18								
					18.38	-0.68	3.66								
					18.97	-1.15	5.38								
192282/6557176	44.77	0.15	-2.20	t, CMUP							45.87	1.71	125.88	77.06	44.62
	35.24	-0.80	-0.22	t, CMX											
192794/2334586	22.54	-0.22	2.73	t, CMUP	45.90	-0.06	1.59				41.66	1.66	211.83	92.58	89.55
	102.26	0.43	-1.29	l											
193029/520988	44.41	0.22	3.02	t, CMUP	51.01	0.82	3.34				37.12	5.83	161.01	87.38	15.72
	43.78	0.46	0.24	l											
194320/41870	88.95	-0.06	1.73	t, CMUP	95.54	0.77	4.95				71.92	0.18	331.27	68.25	121.94
	33.49	1.11	1.53	l	63.35	-0.44	4.02								
					21.60	-1.71	3.25								
194323/3266099	79.37	-0.26	-0.48	t, CMUP	53.01	1.06	3.17				38.18	3.16	211.10	79.55	92.77
	40.93	0.11	0.99	t, CMUP											
194861/612518	77.99	-0.85	-1.48	t, CMX	65.67	0.20	1.59				42.62	1.56	195.89	90.00	78.45
	35.03	-0.13	3.02	t, CMUP	36.36	-0.06	5.29								
194900/173806	75.20	0.33	2.79	t, CMUP	102.51	0.61	0.58				78.84	3.65	311.23	88.51	57.59
	25.45	-0.39	-1.03	t, CMUP	62.80	-1.65	4.35								
	68.02	0.14	0.58	l											
202998/33245	38.78	-0.29	0.39	t, CMUP	69.23	-0.58	3.08				27.01	5.64	143.22	90.87	34.08
	49.71	-1.17	2.78	l	42.36	-1.27	6.06								
203190/159926	55.19	0.03	-3.06	t, CMUP	42.97	1.29	5.65				47.51	1.39	176.08	71.59	62.20
	30.49	0.99	-1.46	l											
203265/14790067	26.89	0.78	2.55	t, CMX							28.26	1.04	95.92	79.02	33.12
	40.78	-0.68	-1.54	l											
203265/4804785	108.26	0.49	-1.20	t, CMUP	59.49	0.05	0.47				106.54	2.62	302.66	110.86	91.64
	16.68	-1.03	1.87	l											

	Leptons				Jets			Photons			$\not\!\!E_T$			Z	
run/event	p_T	η	ϕ	Type	p_T	η	ϕ	p_T	η	ϕ	p_T	ϕ	H_T	M(ll)	p_T
203764/2353176	39.65	0.21	1.81	t, CMUP	164.62	-0.43	4.15				93.75	1.09	263.61	76.81	28.54
	31.20	-0.90	-2.12	t, CMX	97.08	-0.18	0.63								
					16.24	2.03	4.54								
204185/4615893	25.37	0.29	-0.38	t, CMUP	31.13	-0.10	0.86				49.25	0.78	203.14	92.76	86.50
	97.55	-0.33	-2.52	l											
204257/6351843	53.14	0.29	0.32	t, CMUP							31.30	3.67	109.69	75.97	30.85
	25.24	-0.35	3.10	l											
204591/3152942	55.21	0.86	0.01	t, CMX	32.31	-2.38	5.08				25.22	2.27	169.75	90.02	48.24
	41.58	0.19	2.14	t, CMUP	21.11	-1.63	4.34								
					21.45	0.15	2.90								
204722/171103	45.40	0.39	1.02	t, CMUP							41.66	2.97	133.52	96.05	37.50
	46.46	-0.59	-1.29	t, CMUP											
205070/2547391	55.84	0.85	-2.44	t, CMX							27.99	0.65	110.73	77.07	30.09
	26.89	0.85	0.49	t, CMX											
205991/3039577	69.64	-0.23	2.13	t, CMUP							32.67	5.16	128.09	92.64	45.29
	25.78	0.66	-0.74	t, CMX											
206251/588371	24.90	0.99	2.88	t, CMX	128.04	-0.00	2.08				132.05	5.42	389.30	97.12	43.95
	63.45	-0.40	-0.80	l	46.55	0.02	2.56								
206255/1742590	56.49	-0.34	0.05	t, CMUP	44.50	-1.02	3.32				29.44	0.08	169.77	71.96	40.63
	23.46	-0.90	2.53	t, CMX	29.28	-2.20	3.48								
206326/971030	105.32	-0.69	-0.44	t, CMX							114.01	2.96	262.84	109.55	119.89
	43.52	0.24	0.98	t, CMUP											
206326/6047926	35.70	-0.44	1.40	t, CMUP	33.26	-1.79	2.97				25.84	0.34	150.30	91.75	20.61
	55.58	0.06	-1.87	l											
207115/6892740	72.81	-0.10	-3.07	t, CMUP	16.51	0.93	0.72				31.16	0.06	149.50	88.67	55.50
	29.17	0.40	-0.69	l											
209149/1428003	36.15	0.40	-1.49	t, CMUP							25.69	0.01	100.97	92.56	7.95
	39.14	-0.94	1.84	l											

	Leptons				Jets			Photons			$\not\!\!E_T$			Z	
run/event	p_T	η	ϕ	Type	p_T	η	ϕ	p_T	η	ϕ	p_T	ϕ	H_T	M(ll)	p_T
209149/1693283	68.90	0.44	-1.74	t, CMUP							32.43	1.98	141.53	111.13	37.80
	40.21	-0.36	0.93	t, CMUP											
209191/9233196	73.12	0.41	1.66	t, CMUP	83.66	-0.37	5.48				89.04	3.22	278.50	79.20	70.88
	33.02	0.30	-0.21	l											
209372/1881432	72.94	-0.67	1.88	t, CMX	36.05	-1.49	5.04				26.36	4.56	151.33	91.75	44.11
	28.84	-0.62	-1.25	l	15.45	-1.50	0.73								
209848/1141644	52.30	0.86	-1.83	t, CMX							77.12	0.67	172.60	77.15	75.58
	43.17	-0.16	3.13	l											
209920/2592176	33.53	-0.77	3.11	t, CMX							55.90	4.33	163.39	100.83	54.36
	73.96	0.01	0.71	l											
209984/1061083	62.56	0.18	0.41	t, CMUP							53.17	4.26	150.81	88.42	54.65
	35.08	-0.56	2.50	l											
209986/12770713	65.56	-0.27	-2.01	t, CMUP							43.14	2.14	166.43	115.95	44.36
	57.73	-0.03	0.41	l											
209986/4846931	31.39	0.58	1.00	t, CMX	69.74	0.26	2.02				144.65	5.59	345.52	109.52	57.85
	75.42	-0.63	-2.94	l	27.83	-1.50	2.51								
210008/869608	49.76	-0.77	-2.84	t, CMX	90.12	-1.25	0.25				25.11	5.62	128.83	91.15	44.17
	28.92	0.75	1.38	l	50.81	1.91	3.99								
					28.48	1.23	2.71								
211265/6278401	72.89	-0.70	-2.12	t, CMX							67.83	1.81	184.66	100.51	68.93
	43.94	-0.10	-0.15	t, CMUP											
211311/233113	22.56	0.39	-2.65	t, CMUP	33.65	1.52	0.11				42.80	4.78	277.81	90.61	52.27
	105.54	1.18	2.91	l											
	73.45	-0.59	0.19	l											
211452/975147	42.09	0.20	2.28	t, CMUP	46.14	-0.56	5.67				76.64	3.86	226.01	85.62	77.66
	62.46	1.13	0.78	l											

17.2.5 Z + Photon

Table 21: List of "Z + Photon" events. The Z-boson is reconstructed in $Z \to \mu\mu$ decay mode.

	Leptons				Jets			Photons			$\not\!\!E_T$			Z	
run/event	p_T	η	ϕ	Type	p_T	η	ϕ	p_T	η	ϕ	p_T	ϕ	H_T	M(ll)	p_T
177371/273794	34.38 40.32	-0.37 -0.20	-0.49 2.10	t, CMUP l				25.24	-0.34	4.37	6.97	1.44	106.90	71.93	21.04
152507/1700045	66.15 27.68	-0.76 -0.53	-3.00 0.06	t, CMX t, CMUP				34.62	-1.01	0.99	4.48	6.18	146.67	86.05	38.63
162479/90695	46.48 42.52	-0.94 -1.00	1.95 -1.37	t, CMX l	27.58	1.69	3.04	26.73	-0.65	5.99	4.27	0.87	136.75	88.60	8.77
162238/185410	58.38 39.08	-0.29 0.47	-0.12 1.83	t, CMUP l	36.58	-1.11	3.47	28.27	-0.35	4.02	7.26	0.54	169.48	87.12	57.08
167955/33039	55.97 34.76	0.30 0.60	-0.04 2.61	t, CMUP l				26.68	0.58	3.62	2.74	0.34	120.16	86.54	30.26
183915/6947567	112.82 23.05	-0.14 -0.20	-1.27 2.97	t, CMUP t, CMUP				102.27	-0.77	1.71	4.08	6.13	242.23	87.01	104.40
196153/3180853	49.21 48.48	-0.68 -0.90	1.38 -0.84	t, CMX l	55.96	1.09	3.43	38.79	1.06	3.45	17.90	0.68	171.51	88.35	43.15
200309/6273753	57.97 22.52	0.84 -0.63	-2.88 -0.37	t, CMX t, CMX				46.09	0.98	0.75	20.08	4.50	158.23	89.90	41.98
202135/4921851	34.06 60.27	0.37 -1.09	0.35 1.27	t, CMUP l				73.12	0.08	4.09	2.54	4.71	169.99	83.04	85.17
202771/8265405	23.21 77.14	-0.88 -0.96	1.08 -2.00	t, CMX l				59.28	0.88	1.40	7.67	5.29	167.30	84.65	53.99
206697/1401415	28.35 40.73	0.06 0.08	2.59 -0.78	t, CMUP l	44.39	0.23	1.60	29.07	0.22	4.57	2.84	3.70	145.16	67.49	14.74
209265/9524237	50.01 23.11	-0.39 1.18	2.24 -0.50	t, CMUP l				32.72	-0.18	5.18	5.61	1.67	111.45	88.98	30.18
209399/1484144	33.96 33.92	-0.40 -0.55	-0.61 2.40	t, CMUP l	21.41	-2.06	6.12	26.54	-0.27	2.78	6.27	0.50	126.68	67.93	4.52

	Leptons				Jets			Photons			$\not\!E_T$			Z	
run/event	p_T	η	ϕ	Type	p_T	η	ϕ	p_T	η	ϕ	p_T	ϕ	H_T	M(ll)	p_T
209402/10058885	97.31	0.74	0.30	t, CMX	93.96	-0.85	3.32	33.90	0.44	5.38	14.02	3.62	283.10	102.84	117.55
	27.36	-0.90	1.13	t, CMX	34.37	-1.13	3.82								
					26.91	0.88	1.24								